AD-A177 449 THE GAMMA-RAY LASER PROJECT: PROOF OF THE FEASIBILITY OF COHERENT AND INC. (U) TEXAS UNIV AT DALLAS RICHARDSON CENTER FOR QUANTUM ELECTRONIC... C B COLLINS

UNCLASSIFIED JAN 87 UTD-GRL-8601 N00014-86-C-2488 F/G 20/5 NL

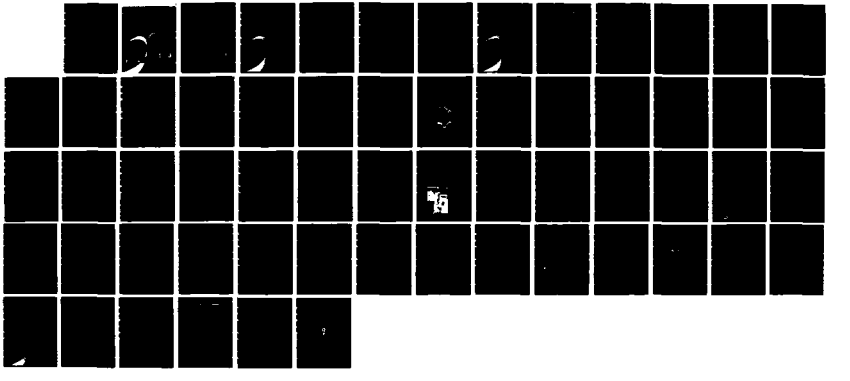

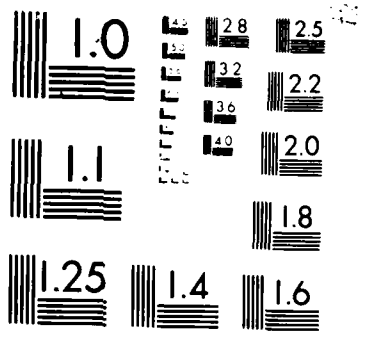

UNIVERSITY OF TEXAS AT DALLAS

(12)

THE GAMMA-RAY LASER PROJECT

Quarterly Report
October–December 1986

(12)

Report GRL/8601

PROOF OF THE FEASIBILITY OF COHERENT AND INCOHERENT SCHEMES FOR PUMPING A GAMMA-RAY LASER

Principal Investigator: Carl B. Collins
The University of Texas at Dallas
Center for Quantum Electronics
P.O. Box 830688
Richardson, Texas 75083-0688

January 1987

Quarterly Technical Progress Report
26 September 1986 through 31 December 1986
Contract Number N00014-86-C-2488

Prepared for
INNOVATIVE SCIENCE AND TECHNOLOGY DIRECTORATE
OF STRATEGIC DEFENSE INITIATIVE ORGANIZATION

Contracting Officer's Technical Representative
Dr. Paul Kepple, Code 4720
Naval Research Laboratory
4555 Overlook Avenue, SW
Washington, DC 20375-5000

SECURITY CLASSIFICATION OF THIS PAGE (When Data Entered)

REPORT DOCUMENTATION PAGE		READ INSTRUCTIONS BEFORE COMPLETING FORM
1. REPORT NUMBER GRL/3601	2. GOVT ACCESSION NO. AD-A177 449	3. RECIPIENT'S CATALOG NUMBER
4. TITLE (and Subtitle) PROOF OF THE FEASIBILITY OF COHERENT AND INCOHERENT SCHEMES FOR PUMPING A GAMMA-RAY LASER		5. TYPE OF REPORT & PERIOD COVERED Quarterly Technical Progress 9/26/86 - 12/31/86 6. PERFORMING ORG. REPORT NUMBER
7. AUTHOR(s) Carl B. Collins		8. CONTRACT OR GRANT NUMBER(s) N00014-86-C-2488
9. PERFORMING ORGANIZATION NAME AND ADDRESS University of Texas at Dallas Center for Quantum Electronics P.O. Box 830688 Richardson, Texas 75083-0688		10. PROGRAM ELEMENT, PROJECT, TASK AREA & WORK UNIT NUMBERS
11. CONTROLLING OFFICE NAME AND ADDRESS INNOVATIVE SCIENCE AND TECHNOLOGY DIRECTORATE OF STRATEGIC DEFENSE INITIATIVE ORGANIZATION		12. REPORT DATE January 1987 13. NUMBER OF PAGES 52
14. MONITORING AGENCY NAME & ADDRESS (if different from Controlling Office) Dr. Paul Kepple, Code 4720 Naval Research Laboratory 4555 Overlook Avenue, SW Washington, DC 20375-5000		15. SECURITY CLASS. (of this report) Unclassified 15a. DECLASSIFICATION/DOWNGRADING SCHEDULE

16. DISTRIBUTION STATEMENT (of this Report)

This document has been approved for public release and sale; its distribution is unlimited.

17. DISTRIBUTION STATEMENT (of the abstract entered in Block 20, if different from Report)

18. SUPPLEMENTARY NOTES

19. KEY WORDS (Continue on reverse side if necessary and identify by block number)

20. ABSTRACT (Continue on reverse side if necessary and identify by block number)

Recent approaches to the problem of the gamma-ray laser have focused upon upconversion techniques in which metastable nuclei are pumped with long wavelength radiation. At the nuclear level the storage of energy can approach tera-Joules (10^{12} J) per liter for thousands of years. However, any plan to use such a resource for a gamma-ray laser poses problems of a broad interdisciplinary nature requiring the fusion of concepts taken from

(continued on next page)

DD FORM 1 JAN 73 1473 EDITION OF 1 NOV 65 IS OBSOLETE
S/N 0102-LF-014-6601

Unclassified
SECURITY CLASSIFICATION OF THIS PAGE (When Data Entered)

20. Abstract (continued)

relatively unrelated fields of physics. Our research group has described several means through which this energy might be coupled to the radiation fields with cross sections for stimulated emission that could reach 10^{-17} cm^2. Such a stimulated release could lead to output powers as great as 3×10^{21} watts/liter. Since 1978 we have pursued an approach for the upconversion of longer wavelength radiation incident upon isomeric nuclear populations that can avoid many of the difficulties encountered with traditional concepts of single photon pumping. Recent experiments have confirmed the general feasibility and have indicated that a gamma-ray laser is feasible if the right combination of energy levels and branching ratios exists in some real material. Of the 1886 distinguishable nuclear materials, the present state-of-the-art has been adequate to identify 29 first-class candidates, but further evaluation cannot proceed without remeasurements of nuclear properties with higher precision. A laser-grade database of nuclear properties does not yet exist, but the techniques for constructing one are currently being developed. Resolution of the question of the feasibility of a gamma-ray laser now rests upon the determination of: 1) the identity of the best candidate, 2) the threshold level of laser output, and 3) the upconversion driver for that material.

TABLE OF CONTENTS

INTRODUCTION 1

Upconversion in the Nucleus 1
Theoretical Context 3
Threshold Estimates 7
Critical Experiments 10

THE SCALING OF FLASH X-RAY DEVICES 15

Motivation 15
Device Design and Construction 17
Operation 20
Performance 25
Summary 29

FREQUENCY MODULATION SPECTROSCOPY 33

Basic Concepts and Phenomenology 33
Instrumentation of FMS 42

REFERENCES 49

APPENDIX 51

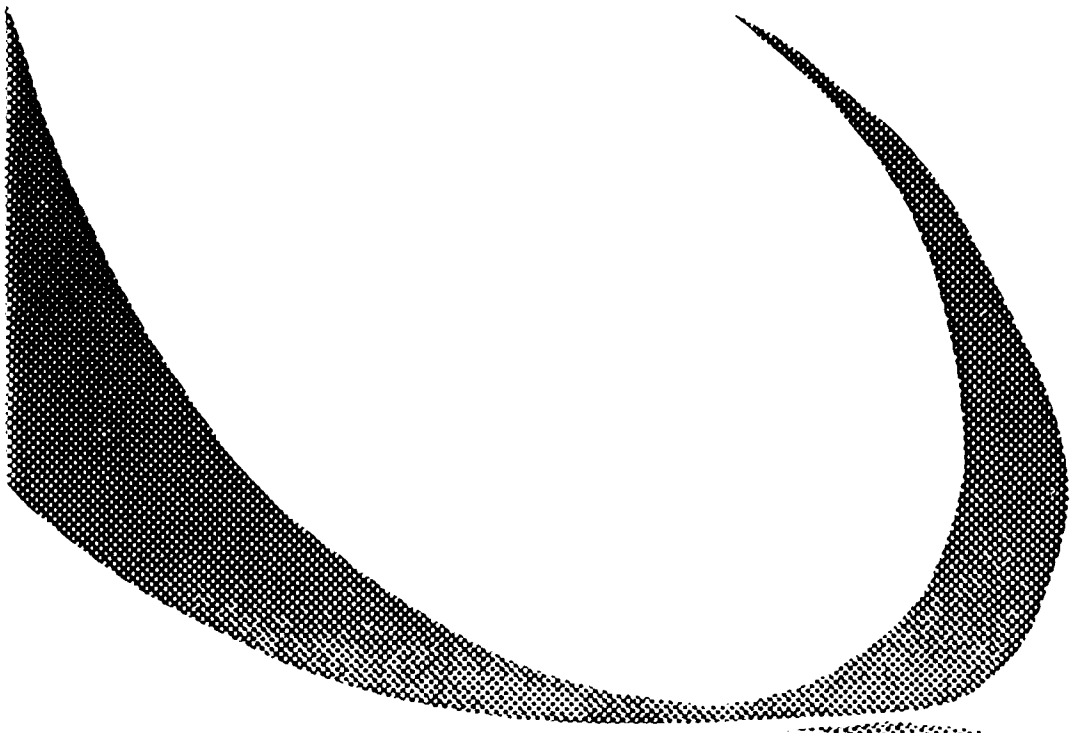

INTRODUCTION

Upconversion in the Nucleus

At the nuclear level the storage of excitation energies in the Mossbauer range of 1-100 keV can approach tera-Joules (10^{12}J) per liter for thousands of years. Over the past seven years, our research group has described[1-16] several viable means through which this energy might be coupled at will to the radiation fields while maintaining the natural Mossbauer width. In such cases the cross section for stimulated emission around 1Å could reach 10^{-17} cm^2, an order of magnitude more favorable than the value for the stimulation of 1.06 μm from Nd^{3+} in YAG. The successful release of such nuclear energies in this way would occur at the rate at which resonant electromagnetic radiation passed through the laser medium and could lead to output powers as great as 3 X 10^{21} Watts/liter. This is an astronomical level of intensity and has not been approached to within five orders of magnitude on earth by any means previously. The peak power from a one liter device would represent 0.03% of the total power output from the sun.

Unfortunately, the quest for a gamma-ray laser has been one of the longest unfruitful efforts in the field of laser science. Virtually all of the sustained pioneering work was done by Baldwin and Solem's groups in the US and by Gol'danskii's in the USSR and focused upon the single photon, brute force approach to pumping. Their work dealt extensively with concepts involving the use of a neutron flux for pumping the laser medium, either *in situ* in real-time, or as a preparatory step to be followed by a rapid separation of isotopes within their natural lifetimes. All proposals were concluded to require infeasibly high levels of particle fluxes to pump the inversions, exceeding even those available from nuclear explosions, and to require neutron moderators having virtually infinite thermal capacities. By 1980 all conceivable variants of the single photon approach had been characterized as hopeless. In 1981 this "traditional" approach to a gamma-ray laser was virtually abandoned with Baldwin's publication of the monumental review[17] of all classical efforts.

The involvement of our UTD Center for Quantum Electronics dates back to 1978, arising from previous activity focused upon fundamental interactions of coherent radiation with matter. Concerned at first with the problem of the correct gauge and basis sets to use in describing multiphoton processes, we began to consider the impact of the work upon areas other than the usual atomic and molecular. As a result, the modernized concept of coherent pumping with optical radiation was introduced in a sequence of papers[1-7] concerned with nonlinear processes mediated by virtual states of nuclear excitation and included the stimulated anti-Stokes scattering of intense but conventional laser radiation.[6] The theoretical treatment served to estimate matrix elements for a new class of two-photon Mossbauer transitions making possible, in principle, the frequency upconversion of optical laser photons to gamma-ray energies.

In 1981 the implications of this theoretical renaissance to the prospects for a gamma-ray laser based on several variants of upconversion were reviewed in an article[3] appearing the following year. If strengthened by recent infusions of dressed state theory,[18,19] that article still provides the most convenient review of the basic concepts and requirements for a viable gamma-ray laser scheme. Subsequently tested in a series of modest experiments, the underlying concepts were confirmed by demonstrating[9-12] that the matrix elements used to obtain the favorable estimates of the threshold for laser output *were correctly estimated* and that extremely large ferromagnetic enhancements of the effective powers applied in the coherent pumping scheme can be obtained. The conclusion from these experiments was *that the gamma-ray laser is definitely feasible if a sufficiently ideal isotope exists in reality.* This is the single most critical issue to the development of a gamma-ray laser--the identity of the most nearly ideal candidate for upconversion.

Despite the many applications of beautiful and involved techniques of nuclear spectroscopy, the current data base is inadequate in both coverage and resolution either to answer the question of whether an acceptable isotope exists or to guide in the selection of a possible candidate medium for a gamma-ray laser. Two new techniques for the measurement of nuclear properties with laser-grade precision have been recently introduced in our laboratory.[20] The full implementation of these techniques has been at the focus of efforts applied during this first reporting period. Detailed in the following material will be the

construction and evaluation of a flash x-ray device for pumping test materials and a Frequency Modulation Spectrometer (FMS) to facilitate the search for certain necessary arrangements of nuclear levels.

Theoretical Context

By involving two distinct steps, the schemes we have discussed[3] for pumping a gamma-ray laser avoid the severe relationships between storage times and spontaneous powers wasted at threshold that were imposed on the single-step processes.[17] Replacement power that is required falls within a technically accessible range avoiding damage to the laser medium.

These two-step, upconversion processes can be divided into two basic categories that correspond to the type of pumping employed: coherent and incoherent, as shown in Fig. 1. The critical concept here is that either transfers the stored population to a state at the head of a cascade leading to the upper laser level. To be effective the pumping processes cannot transfer too many quanta of angular momenta from the fields, and the cascade provides a mechanism for further changes that may be necessary to reach the laser levels. Then the ultimate viability of these pump schemes will depend upon:

1) spectroscopic studies locating a suitable configuration of nuclear energy levels, and
2) "kinetic" studies providing an efficient path of cascading from the intermediate or dressed state to the upper laser level.

A recent variant to the scheme for pumping incoherently with flash x-rays must be mentioned in passing. In it the transfer from storage to intermediate level is assumed to be excited by the direct coupling of energy from giant collective oscillations of electron shells driven by laser radiation focused to power densities comparable to binding energies. While the magnitudes estimated for the gross rates of energy transfer into the nucleus are encouraging, the likely dominance of the inverse process suggests that little net transfer could be realized. Once correlated motion of a shell is established, unless strong processes dephasing the motions of individual electrons are introduced with attendant losses, free induction decay at the end of the pulse will extract the energy back from the nucleus into the fields. This could only be avoided if some super-allowed transition in the nucleus were

assumed to quench the excitation to a lower uncoupled state, but then this is tantamount to the assumption of a type of previously unobserved nuclear transition of very high width. While it is too early for definitive resolution, it is unlikely this recent pumping variant could prove effective and the most likely prospects remain confined to those shown in Fig. 1.

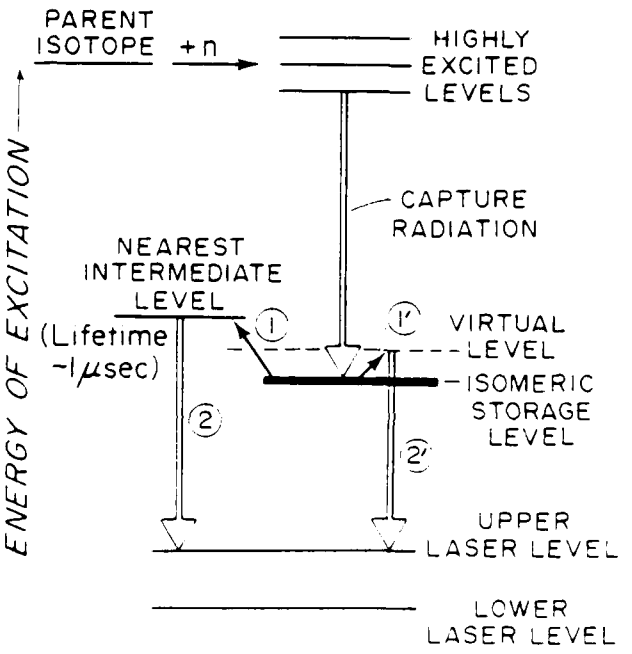

Figure 1: Schematic diagram showing the energetically excited levels of a typical nucleus of interest to the development of a gamma-ray laser. Lifetimes of the stored energies in the isomeric level produced by the initial capture can range from days to hundreds of years. The first phase of the two-step process for the stimulated release of the stored energy is shown in the figure by the solid arrows. Both correspond to the use of longer wavelength radiation to lift a nucleus from the storage level to a higher level of excitation that has a much shorter lifetime. The arrow marked (1) illustrates the incoherent pumping of the storage level through the absorption of an x-ray that is resonant with the energy separation between the storage level and the next higher level of proper symmetry. The arrow marked (1') represents the alternative process of coherent pumping through the non-resonant absorption of a photon from the radiation field in order to create a virtual or dressed state of excitation shown by the dashed level in the figure. In either case the gamma-ray output ultimately results from the upper laser level populated by a cascade occurring as a second step, as shown in the figure by either of the double arrows, (2) and (2').

Because of the interdisciplinary nature of the problem, even for an idealized nuclear material, computations of threshold levels of pumping are not without difficulty. It is useful next to review these fundamental concerns within the context of the nucleus.

From very fundamental bases, the cross section for the interaction of polarized radiation with matter leading to stimulated emission can be generally expressed (even for nuclei),

$$\sigma = \frac{\lambda^2}{8\pi} A g(\nu), \qquad (1)$$

where A is the Einstein coefficient for spontaneous emission and $g(\nu)$ is the normalized lineshape function for the transition attributed to the matter,

$$\int g(\nu)d\nu = 1. \qquad (2)$$

Approximating

$$g_{eff}(\nu) = 1/\Delta\nu, \qquad (3)$$

where $\Delta\nu$ is the absorption bandwidth, we must recall that the actual maximum of $g(\nu)$ is only $2g_{eff}/\pi$.

One intrinsic advantage of gamma-ray interactions is that at the nuclear level the width $\Delta\nu$ is often just the transform of the radiative lifetime. In those cases the Mossbauer effect eliminates recoil and with it problems of thermal motion and Doppler broadening. This natural width gives,

$$\Delta\nu = A/\pi. \qquad (4)$$

Substituting Eq. (4) with Eq. (3) into Eq. (1) yields the Breit-Wigner cross section for stimulated emission,

$$\sigma = \lambda^2/8, \qquad (5)$$

a very large value, even at 1Å. The strongest homogeneous broadening process will limit access to these benefits, but this effect has not yet been observed experimentally. Gamma-ray transitions have been found to have natural widths down to instrumental limits as small as 10^2 Hz. Thus, a lifetime down to at least 1 msec can be safely assumed for a process occurring at 1 Å.

To estimate requirements for the incoherent pumping of populations from a storage level to an upper laser level through absorption of incident x-rays, one further complexity must be introduced. As shown in

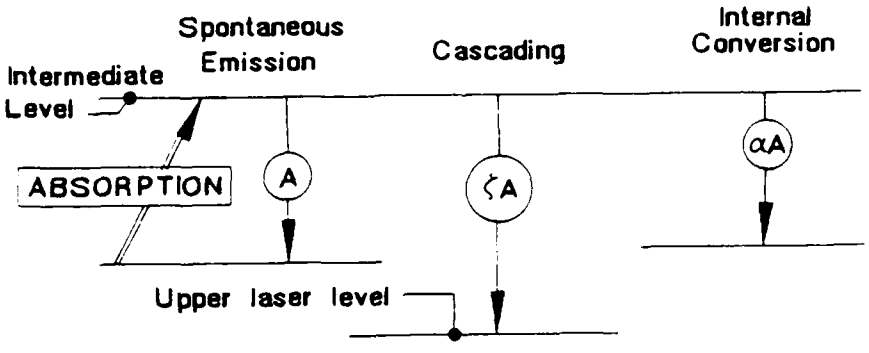

Figure 2: Schematic diagram of both essential and competing processes involved in the pumping of an upper laser level in a nucleus.

Fig. 2, both cascading and internal conversion are accommodated by transition rate coefficients scaled to the A-coefficient by factors ζ and α, respectively. As a result, the total width for absorption becomes

$$\Delta\nu = (1 + \alpha + \zeta)A/\pi, \qquad (6a)$$

while the cross section for absorption is reduced accordingly,

$$\sigma = \sigma_0/(1 + \alpha + \zeta). \qquad (6b)$$

Even with broadening, since the width for a nuclear transition is so much more narrow than the width for any structure in a non-nuclear source of x-rays, the pump must be considered to be a continuum. As a result, the rate of pumping concentration from the initial state is proportional to the product, $\sigma\Delta\nu$ of the terms from Eqs. (6a) and (6b) and is independent of α and ζ (providing broadening is less than 10^{-1}-10^{-} so that σ is not reduced below the cross section for photoelectric absorption by the electrons in the material).

The consequent effects of broadening on the production rates of concentration in various levels at the incident surface of the material is summarized in Table I.

Assuming we pump with both polarizations, a total concentration N can be pumped in the upper laser level,

$$N = N_g F(\nu_g) \frac{\lambda^2 A}{4\pi} \frac{\zeta}{(1+\alpha+\zeta)} \tau_g \qquad (7)$$

where N_g is the concentration of absorbers, and $F(\nu_g)$ is the photon flux per unit frequency averaged over τ_g, the lifetime of the upper laser level. As customarily used, A is summed over the degeneracy, Z_f of the final states and averaged over Z_g initial states so that the Breit-Wigner cross section for absorption must be modified from Eq. (5) through multiplication by (Z_g/Z_f). With that modification, Eq. (7) is entirely consistent with the customary expression for the Mossbauer cross section, as usually expressed when it is recognized the latter describes absorption of a narrow line as opposed to continuum.

Table I

Effect of internal conversion and branching upon production rates of concentrations of levels shown.

Level	Score	Effect	Comment
Intermediate	LOSE	Same production rate	Lifetime over which pump rate can be integrated is reduced by $1/(1+\alpha+\zeta)$
Upper laser level	WIN	Production rate reduced by $1/(1+\alpha+\zeta)$	Usable pump duration is increased up to τ_g, the lifetime of the upper laser level.

Threshold Estimates

The critical concept in the design of a gamma-ray laser pumped by incoherent x-rays is the realization that in Eq. (7) the width-lifetime product, $A\tau_g/\pi$ can be made much greater than unity. In such a case, population from the storage level is funneled through a broad, but short-lived level to a longer-lived laser level for subsequent stimulation. The threshold requirement for the pump flux can be estimated by simply equating the gain contributed by the population pumped according to Eq. (7) with the loss from nonresonant photoelectric absorption from the matrix into which the nuclei are diluted and from the diluent.

In 1982 we published[8] the details of a basic modeling study incorporating this bandwidth funneling in an idealized nucleus. The resulting threshold requirements were accessible to existing technology and were revised even lower with the incorporation of the Borrmann effect, as described at last year's ILS conference[13]. For the output transition, the Borrmann effect allows the development in a crystal of standing waves of such quadrature that coupling to nuclei is enhanced while coupling to electrons is minimized.

Because of recent conflicts in "Private Communications" the actual quantitative level of the enhancement from the Borrmann effect upon threshold requirements is uncertain and the results of last year[13] must be given a larger variance. Current results of the application of Eq. (7) to idealized nuclei diluted to 0.04% concentration in a Be lattice and arranged only for output along a Borrmann mode at 10keV are as follows:

1) Threshold Fluence - 100-300 J/cm^2/0.1%BW/lifetime
2) Temperature Rise - 100-300°C.

Specification of the fluence per unit bandwidth in terms of 0.1% of the transition energy, as shown, is a convenience as it thus roughly corresponds to the fluence within the natural width of an x-ray line.

Estimates of both threshold fluence and temperature rise are extremely sensitive to actual material characteristics. Once the proper nucleus is identified, considerable further improvement is possible. This can be appreciated from the schematic reproduced in Fig. 3 for a typical, but hypothetical case[13]. There it can be seen that the major part of the pump line that is unavailable for nuclear absorption is deposited into the material through the ejection of photoelectrons from a much thicker layer than the one in which the nuclei are pumped. The estimate of temperature rise of 100-300°C. assumes full conversion of the photoelectron energy into heat, but the medium could be layered to permit escape of the primary photoelectrons, thus reducing considerably the temperature rise. An optimal configuration can be arranged once the specific characteristics of the best candidate nuclei are known.

Coherent pumping, the technique depicted in the right of Fig. 1, depends upon the alteration of the properties of the storage level produced by the scattering of large intensities of long wavelength radiation from the nuclei. Again the distinction must be made between

this approach and the recent suggestion to use laser radiation to drive collective but localized oscillations of electrons near nuclei. The concept we address uses coherent, long wavelength radiation to drive the non-local correlations of the electrons manifest as well-known phenomena of magnetization or ferroelectric polarization throughout the bulk of the material.

In ferromagnetic and ferroelectric hosts the active nuclei are immersed in extremely large fields capable of developing substantial interaction energies across a nuclear volume when switched by relatively modest applied fields. If transitions to the storage level exist in the nuclei at energies comparable to that of a photon of the driving fields, the properties of the other state of the transition will be mixed into those of the storage level. It is assumed that this other state is better able to radiate gamma radiation. While the driving field need not be precisely resonant with the transition energy, the detuning, ΔE from resonance must be comparable to the interaction energy if properties are to be fully mixed. In such cases, the metastability of the storage level against gamma-ray emission is switched off by the admixture of properties from the other state of the low energy transition

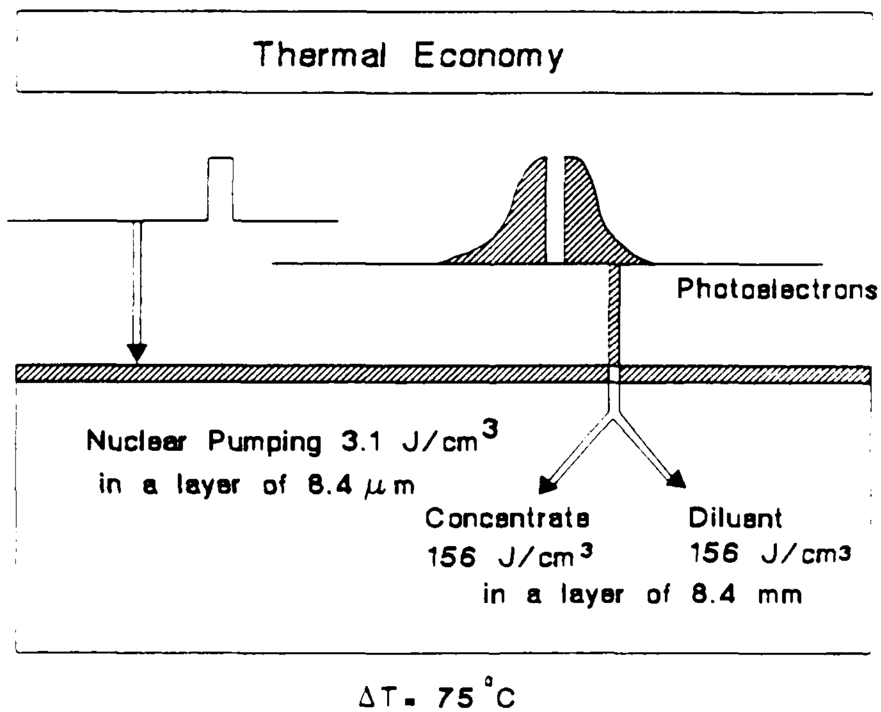

Figure 3: Schematic diagram of the thermal economy of the scheme for pumping a gamma-ray laser with broader band x-radiation.

being driven. It is this concept which comprises the foundation of the scheme for coherently pumping a gamma-ray laser.

While precise computations of the threshold for coherent pumping are not yet available, estimates from perturbation theory[3,16] suggest that the threshold requirements in idealized cases are comparable to those presented above for the case of incoherent pumping. The principal difficulty in this case is that, again, estimates are extremely sensitive to material specifics. For coherent upconversion to be viable, a real nucleus must be found with two accidentally degenerate levels, one being a long-lived isomeric state. Such a combination would be completely invisible to current techniques of nuclear spectroscopy.

Critical Experiments

Under the idealized conditions discussed above, the part of the pump energy which must be supplied *in situ* would not be large enough to represent a major impediment to the realization of a gamma-ray laser. The real difficulties take peculiar forms. The use of coherent upconversion would require the location of nearly degenerate levels which could not be resolved by conventional techniques of nuclear spectroscopy. The use of incoherent pumping with x-rays would require a level of knowledge about branching ratios and transition probabilities beyond that available from current methodology. In fact, the paucity of laser-grade data describing nuclear properties is so severe that one cannot say which real isotope represents the best approximation to the ideal.

For lifetimes ranging from seconds to infinity there are 1886 real nuclei to consider as candidates for a gamma-ray laser. Our computer based searches of the existing data base have served to identify 29 first class candidates. Of these, 10 are known to have the necessary (but not necessarily sufficient) arrangement of levels in which there is an isomeric storage level and at lower energies: 1) an upper laser level with lifetime between 1 nsec and 10 μsec, and 2) a lower laser

level of even less energy. For these materials, the applicability of the favorable threshold estimates will depend upon:

1) spectroscopic studies locating a suitable intermediate or scattering state to which transitions can be made from the isomer, and
2) "kinetic" studies providing an efficient coupling from the intermediate or scattering state to the upper laser level.

To meet this need for laser-grade data on nuclear properties we recently introduced[14-16] analogs to the powerful techniques for evaluating spectroscopic and kinetic properties of atoms and molecules at optical wavelengths. These are shown schematically in Fig. 4.

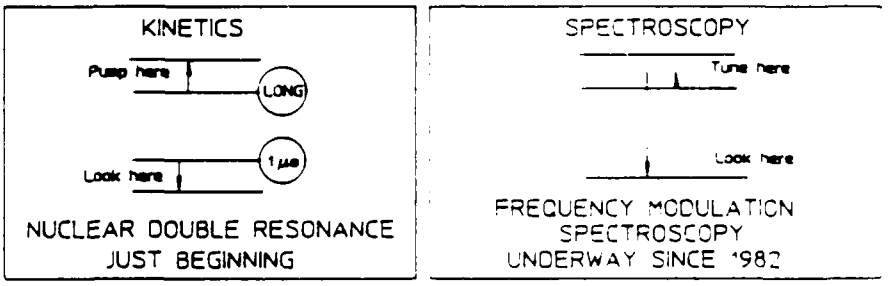

Figure 4: Schematic representation of nuclear analogs of the optical double resonance and Raman spectroscopic methods that have served so effectively to build a laser related data base for atomic systems at optical energies.

Essential to the success of the double resonance experiments is the accessibility of a source of pulses of x-rays of nanoseconds duration that is very powerful in comparison with conventional devices. A fluence from the pump of 10^{-6} keV/keV of bandwidth is needed in a reasonably brief working period. Either laser plasmas or large e-beam machines can do this in a single shot, each of which requires about an hour of laboratory time to prepare; but costs are very high. As a result, none of these traditional light sources for the subAngstrom region could be used to complete an evaluation of the 29 most attractive materials before the turn of the century.

In the following section we detail the most recent [illegible] with a prototype flash x-ray device[17], FALCON which can emit 3 kW average power near 0.5Å. A Blumlein driven device, it apparently is one of the first which is not choked at the output diode. Reasonable matching of beam to

line allows pulse durations to be as short as 20 ns c with peak powers reaching 150 kW. About one-third of the pulse energy appears in the K, lines of the anode material, meaning that at those particular energies, outputs approach the design objective of the ALS synchrotron configured with the 13.6 wiggler, as shown in Fig. 5. Linewidths from FALCON and the ALS with wiggler are comparable, but of course the ALS output is collimated and tunable to any energy within the envelope while lines from our device are fixed at the K-line energies of available anode materials. However, costs of our table top device are three to four orders of magnitude less and for the illumination of extended absorbers it offers an interesting alternative to the more conventional sources of x-rays.

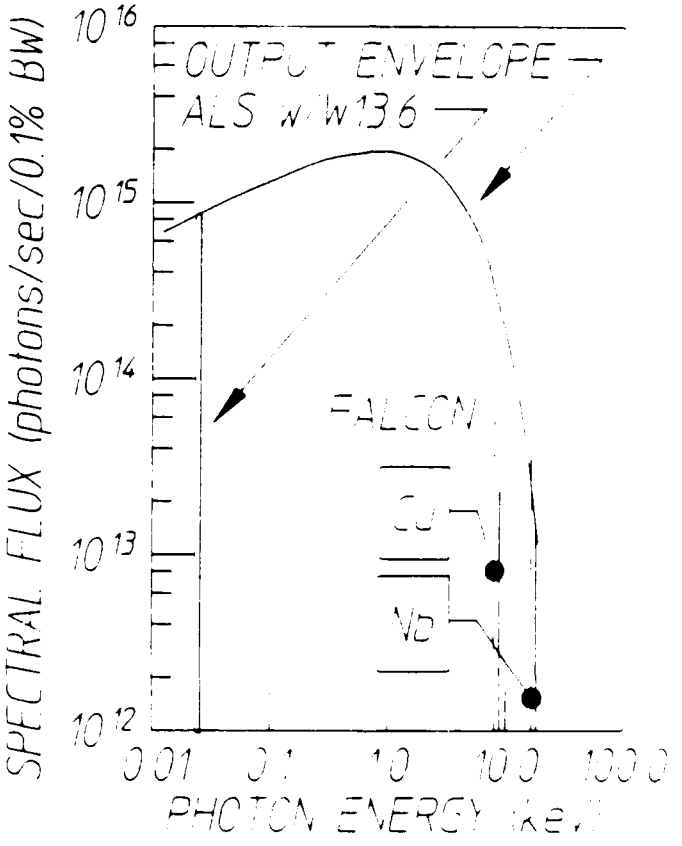

Figure 5: Spectral flux from our Blumlein driven, flash x-ray device, FALCON, in comparison to the design objective of the ALS synchrotron with a 13.6 cm wiggler. Line output is determined by the composition of an interchangeable anode and two examples are shown.

Perhaps of greater interest is that 2/3 of the output energy in each pulse from FALCON is distributed in a true continuum in which all wavelengths in a range from about $E(K_\alpha)$ to about $\Delta E(K_\alpha)$ are present. It considered as equivalent to a pulsed radioactive source, when "on," each pulse is the equivalent of [illegible] of strength within the energy [illegible] allowed nuclear transitions, simultaneously at every possible transition energy in the range. Since energies of potential pump transitions in most systems are very poorly known, the availability of continua from FALCON actually makes it a more viable source for mounting double resonance experiments, than would be a synchrotron which would have to be tuned over the working range, line at a time.

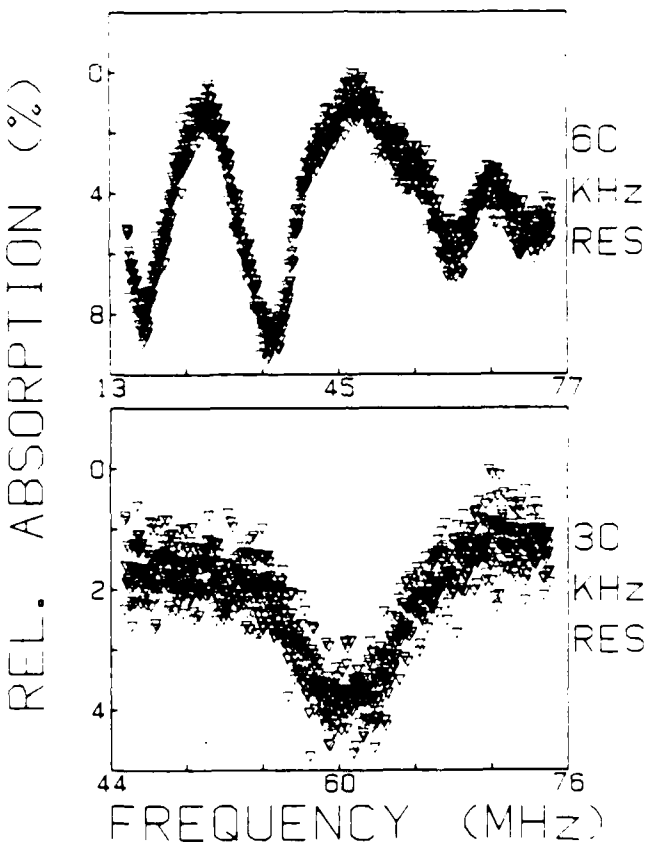

Figure 6. First continuously tuned FMS spectrum of a nuclear material, in this case the 14.4 keV transition of the simulation nucleus ^{57}Fe. Instrumental resolution is indicated and observed linewidths correspond to the transform of the lifetime of the nuclear state.

The other new technique of Fig. 4 preserves the high resolution aspects of Mossbauer spectroscopy but replaces the mechanically generated Doppler shifts, conventionally used for tuning, with sum and difference frequencies generated by a mixing process. A computer controlled frequency synthesizer sweeps a radiofrequency used to switch intense magnetization in a host material into which the test nuclei are diluted. Tunable sidebands generated on the intrinsic gamma-ray transition then replace the Doppler shifted lines as probes.

The first spectrum from such a continuously tuned Frequency Modulation Spectrometer (FMS) is shown in Fig. 6 to be unexpectedly rich in detail. Not a laser candidate but a simulation, ^{57}Fe was used in this demonstration. Shown in absorption are resonant structures from expected states in the lower panel together with unexpected surface states, yet to be analyzed. Widths of the lines are not instrumental but rather reflect the transform of the lifetime of the final state of the nuclear transition at 14.4 keV.

Detailed review of both new experiments is presented in the following sections and testifies that momentum is building in the development of new technology necessary in the search for the best candidate material for a gamma-ray laser.

THE SCALING OF FLASH X-RAY DEVICES

F. Davanloo, T.S. Bowen, J.J. Coogan, and C.B. Collins

Motivation

The developing availability of synchrotron light sources has stimulated many areas of research requiring pulses of radiation in the x-ray region. Average x-ray powers can now be great enough so that many experimental responses can integrate above the noise in reasonable working periods. Unique features such as the collimation of the output seem to render the synchrotron irreplaceable for many applications. Nevertheless, the imbalance between demand and the supply of such facilities motivates the development of alternative sources for at least some of the applications which do not need all of the distinctive features of the synchrotron. One such application of vital interest to the gamma-ray laser project lies in examining the nuclear fluorescence from candidate materials irradiated by x-rays in the 1-100 keV range of energies.[3] Since we are using extended absorbers, collimation is not important. For us the essential figure-of-merit lies in the average x-ray power emitted over the bandwidth of interest in pulses of duration of the order of 10 nsec or less.

While both laser plasmas and large e-beam discharges offer alternative solutions to the need for maximal emitted power in the x-ray region, those also are large and expensive devices requiring complex supporting facilities. A first major step in the realization of a laboratory scaled, pulse x-ray source was the Blumlein-driven generators of Bradley[23] and co-workers.[24] For pulses as short as 100 nsec their device performances have succeeded to the point limited by fundamental considerations,[23,24] while the apparatus remained portable and self-contained. Nevertheless, those generators, together with the laser plasmas and e-beam devices, were characterized by very low repetition rates which would necessarily limit their usefulness in experiments dependent upon the integration of responses that occur with low probabilities.

Recently we reported[22] a further step in the realization of a laboratory scaled alternative to the synchrotron for some applications.

We described a Blumlein-driven x-ray diode for which impedances had been controlled to yield output pulses of about 10 nsec duration with reasonable efficiency. Moreover, commutation was effected with a hydrogen thyratron so that operation to high repetition rates could be realized. At 100 Hz an average x-ray power of 35 mW was reported. Here as a result of first quarter activities we describe the scaling of this type of device to yield 300 mW of x-rays while retaining its table-top aspects. For comparison, the design objective[25] of the Advanced (synchrotron) Light Source, ALS, is to produce an x-ray power integrated over all wavelengths of only about one order of magnitude more. Thus, it seems that unless the unique advantage of collimation is essential to a particular application, the laboratory scaled system we designed specifically for our application can offer attractive support for many other experiments that would otherwise require the availability of a synchrotron.

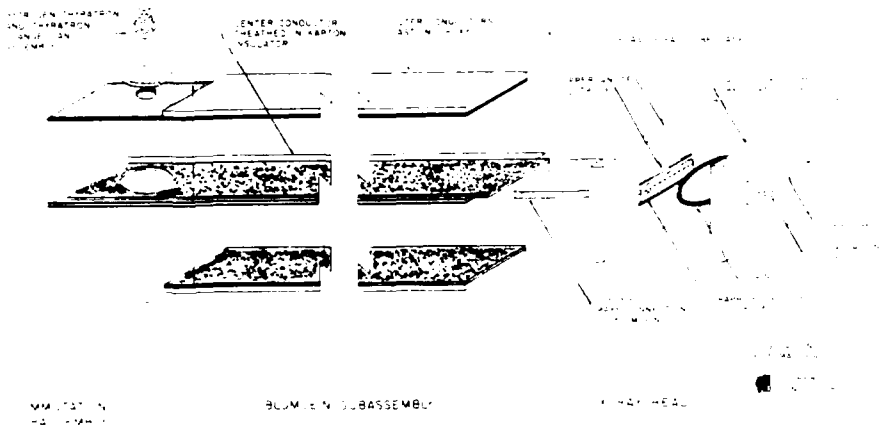

Figure 7: Schematic drawing of the high repetition rate, flash x-ray device characterized in this work.

Device Design and Construction

As described in our previous report,[22] the design of our flash x-ray device centers around three critical subassemblies:

1) a low-impedance x-ray tube,
2) a Blumlein power source, and
3) a commutation system capable of operation at high repetition rates.

This basic organization was shown in our first report[22] in a schematic that is reproduced in Fig. 7 for convenience. Elements (2) and (3) differed little from drivers we had developed earlier for short pulse nitrogen ion lasers.[26]

For the initial investigation of the scaling of this flash x-ray device to higher powers, two larger systems were constructed: one with a nominal, 1.8Ω line capable of storing about 7J, the other with a 0.85Ω line storing 8J. Because of the thicker dielectric layer giving the larger impedance, the first was capable of routine operation at higher voltages. In both cases the Blumlein was constructed from massive copper plates, potted with epoxy on outer surfaces to reduce corona, and separated by layered Kapton (polyimide) dielectrics. In operation, the middle conductor was charged to a positive high voltage which could be varied to 30 kV and commutation was effected by an EG&G 3202 hydrogen thyratron mounted in a grounded grid configuration. The average

TABLE II

Comparison of the dimensions and parameters of the Blumleins in the three devices used in these scaling studies.

System	0	A ("scale 0.33")	B ("EXRAD")
Dielectric	Layered Kapton and epoxy	Layered Kapton and epoxy	Layered Kapton and oil
Thickness	0.66 mm	0.69 mm	0.38 mm
C(storage)	3.2 nF	7.2 nF	9.5 nF
C(switched)	3.5 nF	8.7 nF	9.1 nF
Line impedance	1.8 Ω	1.8 Ω	0.85 Ω
Transit time	5.5 nsec	11.4 nsec	6.8 nsec

available input power was sufficient to support operation to a 100-Hz repetition rate in most configurations. Comparative values of line dimensions and parameters are summarized in Table II together with a description of the earlier system in the first column.

Charging of the Blumlein was accomplished with one of two alternative systems, a d.c. power supply or a resonantly pulse charged source. The latter configuration is shown schematically in Fig. 8, together with a typical timing sequence of operation. Advantages accrued to the pulsed charge system because it was physically more compact and because of the lessened duration over which high voltage stress was applied to the Blumlein insulator. However, with either power supply the integrated x-ray device could be operated to 30 kV in air in a table-top mode.

With emphasis on obtaining a singularly low inductance input to electrodes designed to give a filamentary source of radiation, the x-ray tube was constructed from cast materials, selected to minimize erosion and maximize heat transfer. Copper foil strips 0.05 mm thick and 10 cm wide were fastened to the electrode mounts and were then passed through

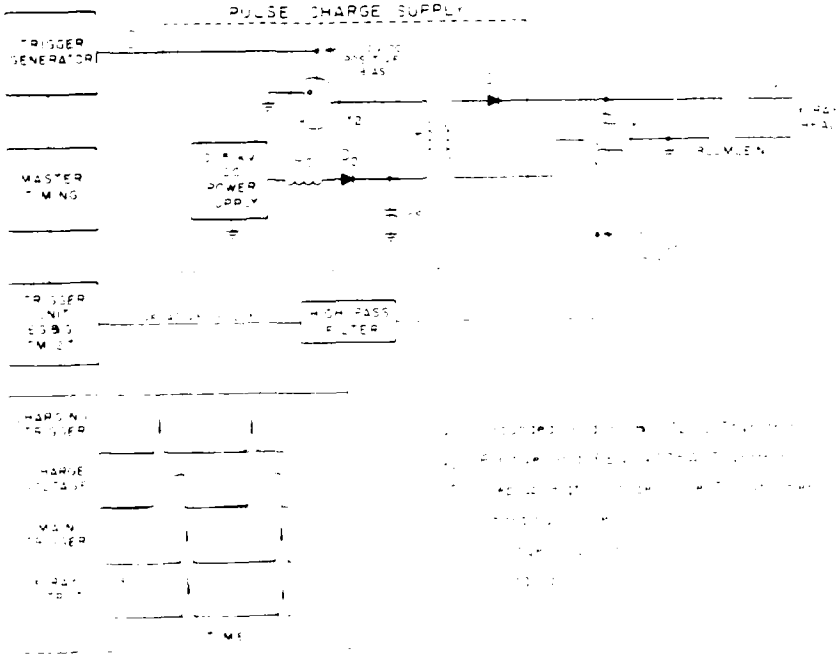

Figure 8 Resonant pulse power supply used to charge the Blumlein in these experiments. The inset shows a typical timing sequence and the relationships between various events essential in the device operation.

the cast material forming the base of the x-ray head before it hardened. After emerging from the base, the foils were joined to the outermost copper plates of the Blumlein. In this way any transverse constriction of the path of the discharge current between the Blumlein and the electrodes was avoided.

The design of the x-ray tube for these scaling studies has evolved substantially from that used in the first models reported earlier.[8] In that earlier system the anode had been cast directly into the material forming the base to facilitate passage of the connecting foil through the base. In that design the x-ray tube was considered to be an expendable component and the cost of construction was low enough to justify that conception. However, a recent refinement of objectives has created a potential need for the use of exotic metals and it became necessary to develop the capability shown in Fig. 9 for the interchangeability of anodes. In this design the anode is a simple cylinder of metal, 6.35 mm in diameter and 10 cm long which is inserted into a socket as shown. The cathode was demountable, as well. As in the

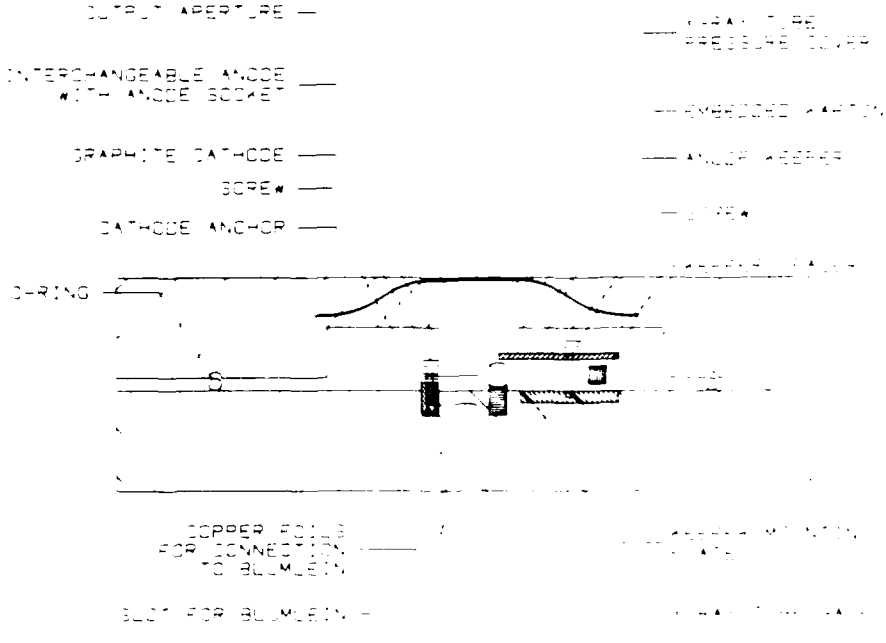

Figure 9. Schematic drawing of a cross section of the x-ray diode used in this work emphasizing provisions for interchanging materials used as anodes.

disposable version, it consisted of a strip of 0.381-mm-thick graphite further ground with a blade-like edge 10 cm wide and separated from the anode by a variable distance chosen to optimize performance. The electrical length of the strip was selected to give a resistance that was comparable but below the line impedance in order to assist in damping the ringing of the discharge current at times subsequent to the initial pulse which produced the x-rays. The position of the line of intersection between the midplane of the current sheet and the anode surface proved to be an important parameter most probably because of a potential compensation between the angular distribution of the emitted x-rays and the possible shadowing effect of the body of the anode rod for some relative positions. To optimize this geometry shims were inserted to raise the cathode blade in order to maximize the output.

The discharge space was enclosed by a pressure shell, also fabricated from cast materials with an integral window of 0.076-mm-thick Kapton plastic film. The window aperture was covered with a graphite plate 0.127 mm thick to eliminate the emission of visible and UV light. Even with the cast construction and ready access to internal electrode spacings, operating pressures below 3.0 mTorr were routinely maintained with a small mechanical pump. Performance was not noticeably dependent upon the residual pressure in the x-ray tube unless it rose to approach 10 mTorr, a value near which outputs were abruptly quenched.

Operation

Precise measurements of time-resolved voltages and currents were rendered difficult by the extremely low impedance of the Blumlein and by the commutation of the thyratron in a grounded grid configuration on this particular decade of time scales, 1-20 nsec. With resonant pulse charging of the Blumlein it was possible to shunt the x-ray tube with a voltage divider constructed from a tapped water resistor of a sufficiently low impedance around 200Ω, so that meaningful measurements of voltage as a function of time could be made with limited radio frequency interference (RFI). Sampled voltages were suitably attenuated upon entry into a heavily screened room where they were recorded with a Tektronix 7912AD transient digitizer. Precautions notwithstanding, there remained sufficient RFI to introduce triggering jitter of about ±10 nsec whenever absolute timing of signals was attempted.

Operation generally produced the switching waveforms of voltage expected of such Blumleins[26] with the charge voltage and the discharge gap separation emerging as the two most critical experimental variables. Figure 10 shows the dependence of the voltages measured across the x-ray diode as functions of time for the various spacings of anode to cathode indicated there for a charge voltage of 22 kV. In contrast to earlier impressions,[22] it can be seen in Fig. 10 that significant voltage multiplication does develop before enough current is discharged through the x-ray diode to limit further ringing of the voltage to even higher values. For electrode spacings producing useful amounts of x-rays the peak voltages typically reached values of 1.3 to 1.5 times the charge voltage originally applied. Also seen clearly in Fig. 10 is the extent

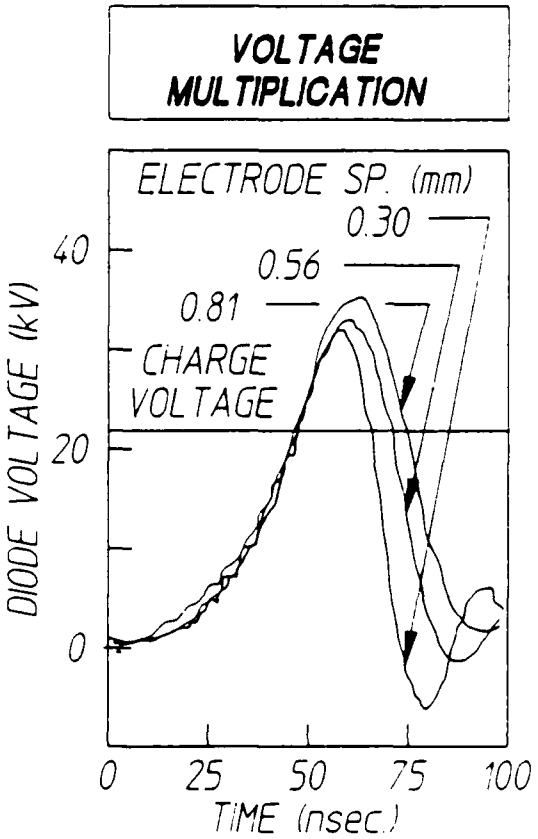

Figure 10: Voltages measured across the electrodes of the x-ray diode driven by system B as functions of time for the various spacings of anode to cathode indicated. Charge voltage of the Blumlein before commutation was 22 kV.

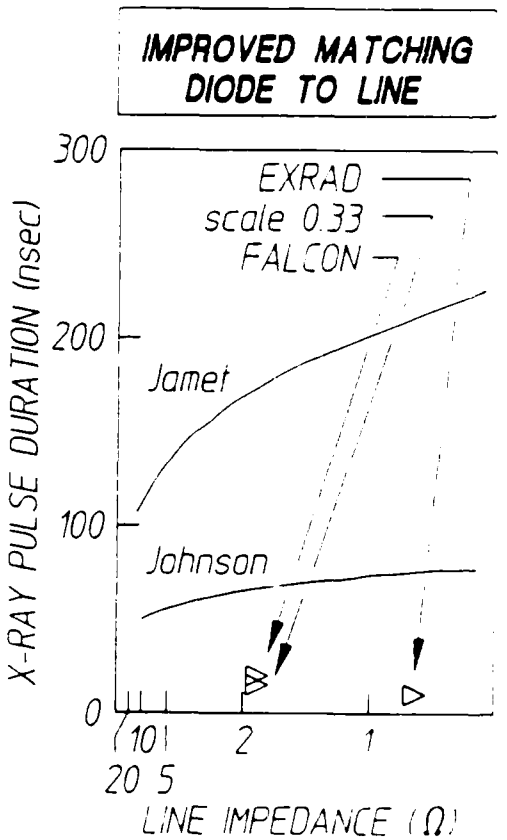

Figure 11: Combinations of Blumlein impedance and x-ray pulse duration displayed by devices constructed in this quarter. For comparison the solid lines plot the ranges of parameters spanned by earlier sources described in the review of Ref. 27.

to which smaller discharge gaps facilitate the earlier initiation of the "switching" portion of the waveform during which the multiplied voltage is rapidly falling and as the current is presumed to be rising.

In contrast to earlier pulsed x-ray devices described in the literature,[27] the systems we report are apparently the first not choked at the head. The extremely low profile of the x-ray diode resulted in an effective impedance of about 1-2Ω at the frequencies characteristic of those in the voltage waveform. Thus, the diodes were reasonably well-matched to the Blumlein during the most important part of the discharge of the current. As a result, the output pulses were found to have durations comparable to the transit times of the lines, an aspect not seen in previous devices. In fact, the combination of pulse duration and line impedance represents entry into a new region of parameter space, as shown in Fig. 11.

X-ray outputs were detected with three different systems. Measurements of absolute pulse energies utilized a moderately fast scintillator plastic equivalent to NE114 with nominal 7.0-nsec decay time. The resulting light output was detected with a photomultiplier having 1.5-nsec resolution and integrated with an EG&G/Ortec charge sensitive preamplifier. Calibration was obtained by comparing the time-integrated fluorescence from the plastic detector when illuminated with geometrically attenuated x-rays from the flash source directly with the level of excitation produced by a radioactive source of known characteristics. This technique was used to determine the dependence of the total energies in the x-ray pulses as functions of the important experimental variables.

More direct measurements of the time dependent evolution of the output intensities were made with the other two detector systems. In one the scintillator in the above system was replaced with a faster plastic equivalent to Pilot-U with a nominal 1.36 nsec decay time and the photomultiplier anode signal was input directly to a Tektronix 7912AD transient digitizer. Numerical deconvolution was subsequently employed to remove the combined time constants of the photomultiplier and plastic. Attention to the reconstruction of the baseline after deconvolution enabled an empirical time constant of 3.5 nsec to be identified as being the most probable value in reasonable agreement with

the sum of the manufacturer's specifications cited above. Confirmation of the temporal dependence was obtained with a Hamamatsu Type S1722 PIN diode with 1 nsec risetime connected to the Tektronix 7912AD digitizer without preamplification. While this last system proved preferable for the study of the dependence of the relative intensity upon time, long-term drift of the rather low sensitivity together with the absorption in the window made it difficult to use for the routine determination of absolute intensities.

Figure 12 shows the results of a typical measurement of the output intensity as a function of time from system B that was made with the PIN diode, cross-calibrated with the scintillator plastic to obtain the absolute scale of intensities. Comparable data taken entirely with the scintillator/photomultiplier combination agreed completely with such data but displayed a greater level of noise. Seen clearly in Fig. 12 is the comparable effect on x-ray output seen in Fig. 10 for the voltage developed across the x-ray diode. Operation with smaller separations between anode and cathode resulted in earlier termination of the period

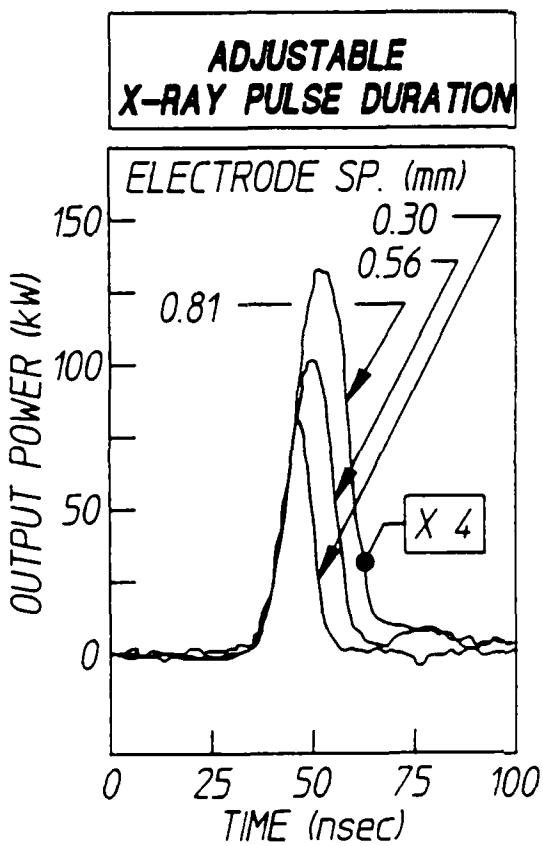

Figure 12: Typical dependence of output x-ray power emitted by system B as a function of time for the different electrode spacings shown. Charge voltage of the Blumlein was 22 kV.

during which power was effectively transferred to the load at a sufficiently high voltage to accelerate electrons to the energies needed to excite x-ray emission from the inner shells of the atoms of the anode material.

Figure 13 shows the relative times at which switching and x-ray emissions were found to occur. As mentioned earlier the triggering was not entirely stable; however, it did not vary continuously but rather alternated among several discrete positions. The data of Fig. 13 was obtained by selecting on the basis of histograms the most probable

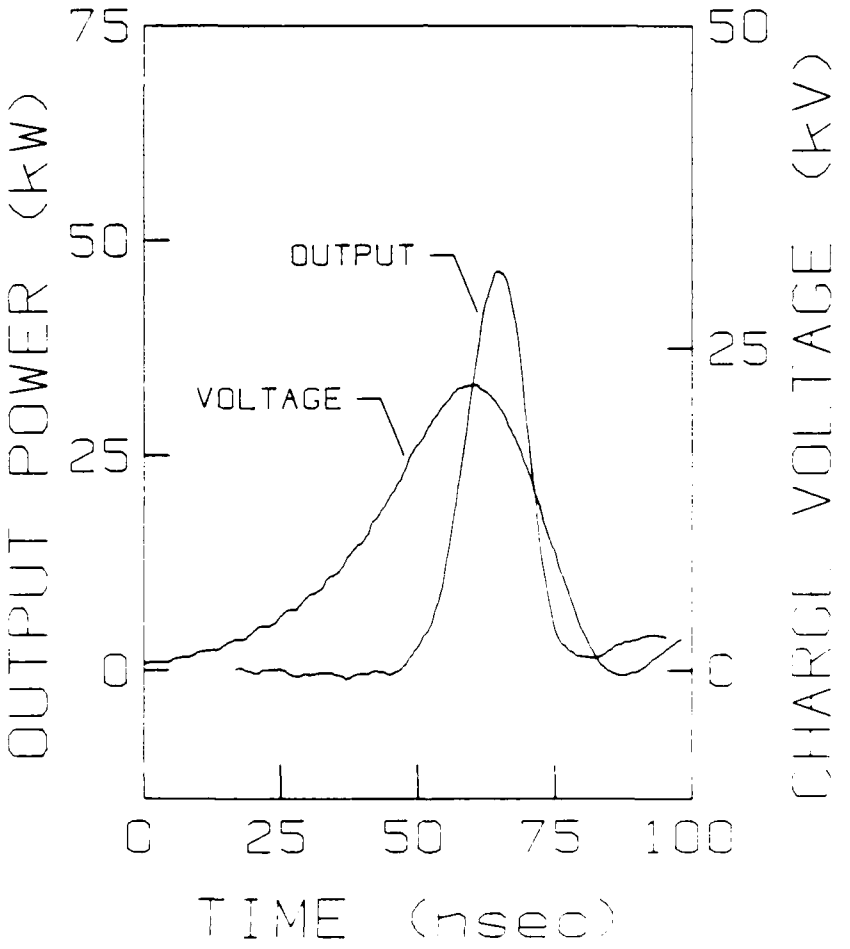

Figure 13: Typical relationship for the voltages and output intensities measured at the x-ray diode. These particular data corresponded to a charge voltage of 22 kV applied to an electrode spacing of 0.56 mm by system B.

waveforms. The resulting standard deviation of the timing skew between the curves shown in Fig. 13 was 3.1-nsec.

For each of the three devices examined in this first phase, the x-ray fluence delivered to an external target could be visually examined for uniformity under both single pulse and higher repetition rate conditions by allowing it to fall upon a fluoroscopy screen of the type used in radiography. A uniform pattern, sharply delineated by the edges of the output aperture, could be readily seen to result from the great majority of discharges. Pinhole photographs of the output orifice showed the actual origin to consist of a largely uniform distribution of densely packed sources along the length of the anode. Resolution was sufficient to show that the emission occurred primarily from the region between the anode and cathode, presumably from vaporized anode material being accelerated toward the cathode. Operationally the x-ray head was equivalent to a fast linear flashlamp in the x-ray region.

Performance

For each of the devices characterized in this work, there was found to be an optimal value of anode to cathode spacing. Figure 14 shows the typical variation in x-ray pulse energy observed as that separation was changed. Such data presented the same general trend, thus refining the impression given in the preliminary report.[2] The trend displayed in

Figure 14: Total x-ray pulse energy emitted near 1Å under single-shot conditions (1.4 Hz) as a function of the separation between anode and cathode. These particular data were obtained from a Mo anode operated in system A initially charged to a voltage of 28 kV.

Fig. 14 at smaller values of electrode spacing was entirely reproducible in this work and is readily comprehensible in the context of Figs. 10 and 12 showing a decreasing pulse width to result from more narrowed separations.

To within a few anomalies discussed below, the output energies, E emitted at the optimal electrode spacing for a particular system scaled as

$$E = AZV^3 \qquad (8)$$

where Z is the atomic number and V the accelerating voltage, in general agreement with algorithms describing the intensity from traditional continuouswave (cw) x-ray tubes operating at constant current at voltages reasonably above threshold, when adjusted for the fact that in these devices current is proportional to V. Figure 15 illustrates this behavior for operating voltages sufficiently above threshold.

The scaling of x-ray outputs to larger values with increased system size is also shown in Fig. 15. In addition to the two larger devices

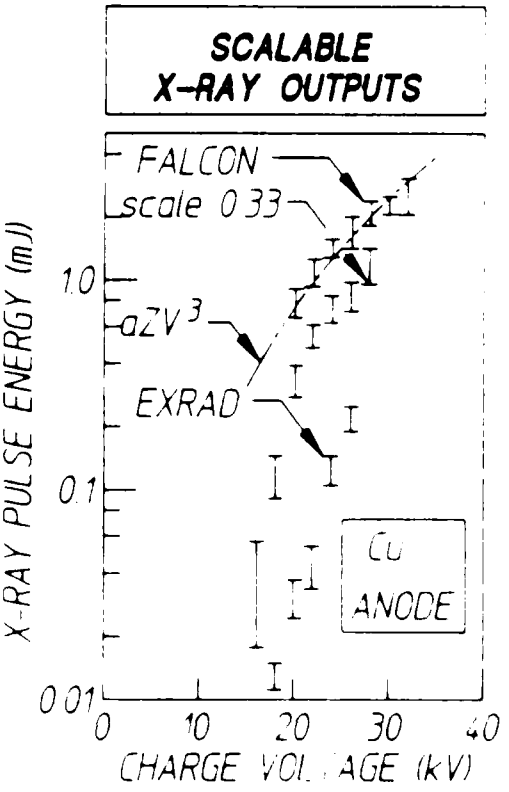

Figure 15: X-ray pulse energies emitted as functions of the charging voltage of the Blumleins for two of the three different systems in Table II, together with a larger scale device, FALCON

described in Table II, the outputs from FALCON, a large scale system, are shown in Fig. 15. The basic scale is set by storage capacity which was nominally in the ratio of 1/3/10. A photograph showing two of the FALCON class devices is shown in Fig. 16. In future operation the Blumleins will be lowered into the oil bath on top of which they rest in the photograph.

With the larger devices considered in this work x-ray pulse energies were found to remain largely constant as the pulse repetition rate was varied over the range from 1 to 200 Hz. Figure 17 shows this to be reflected in the measured values of average power output in the x-ray pulses from the largest of the devices. Limitations imposed by the primary power supply to the pulse charge system prevented the actual operation simultaneously at both the maximum values of repetition rate and at voltages higher than shown in the figure. However, the absence of any significant variation in output pulse energy with repetition rate indicates from Fig. 17 that average powers in excess of the 300 mW shown

Figure 16. Photograph of two of the FALCON class flash x-ray devices.

are readily within the capabilities of these devices. Each data point in Fig 17 was the average of a sequence of measurements and the highest power recorded in this way was 300 mW for system A at 28 kV and 200 Hz.

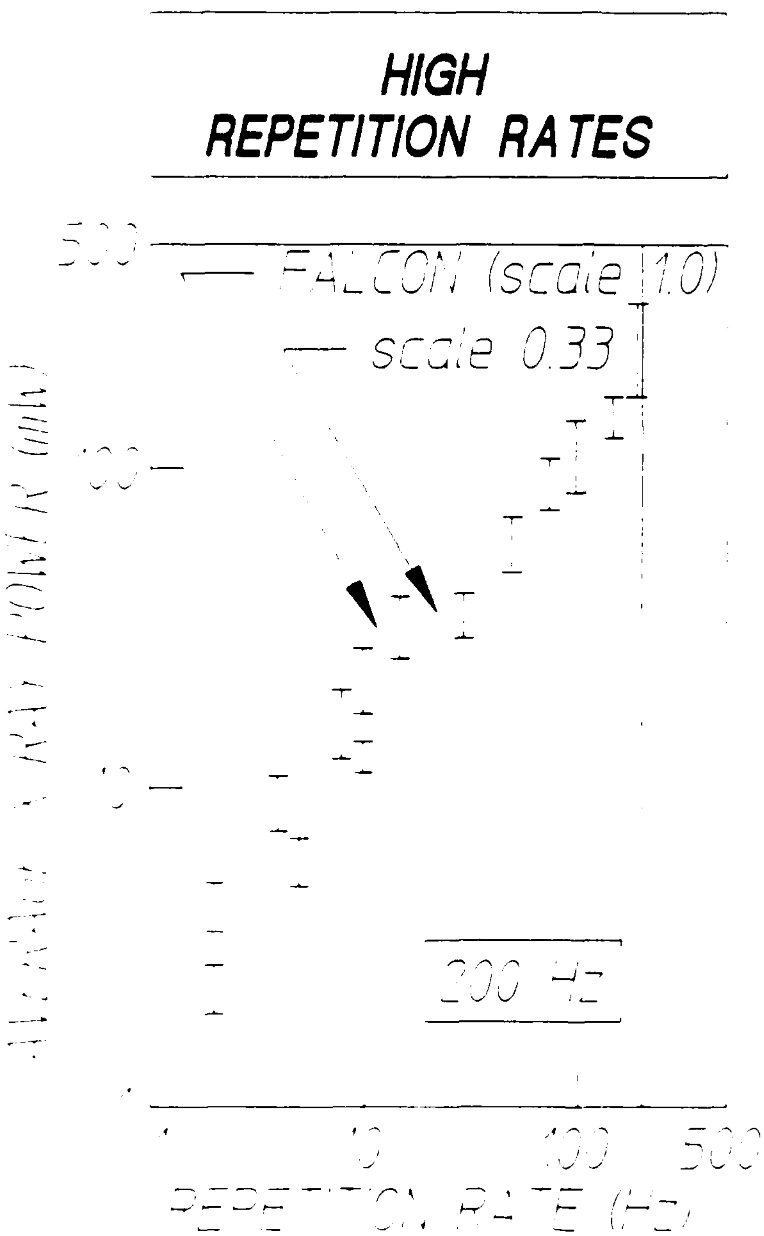

Figure 17: Average powers emitted as x-rays near 1Å as functions of the pulse repetition rates for charge voltages of 28 and 26 kV onto the smaller and larger systems shown.

Measurements with a Si-crystal detector located at such a large distance that only one photon was recorded per pulse showed the energies to be emitted into both K-lines from the anode material and continuum. A third of the energy was found in the K-lines leading to spectral fluxes summarized in the introductory section of this report. Of great significance is that the remainder is distributed over a fairly broad band of true continua as shown in Fig. 18. This continuum will be extremely important for the pumping of that majority of candidate materials for which transition energies are poorly known.

Summary

The results of this quarter's efforts in developing laboratory scale sources for pumping candidate materials for a gamma-ray laser are summarized in Table III. Listed there are the surprisingly large values of equivalent radioactivity to which these outputs correspond. Strengths of nuclear sources of pump radiation are traditionally measured in Curies (Ci). For scale, a large device for cancer therapy may be a few kiloCuries distributed into a few (<10) linewidths but such sources can only be pulsed with relatively slow mechanical shutters. Reported here has been the successful demonstration of full-scale, flash x-ray sources of radiation for the 3-30 keV range of energies. They produce 20 nanosecond pulses of up to 6800 MegaCuries peak strength emitted into a continuous distribution of the linewidths that fills the range of potential interest without gaps. This is 27 Ci instantaneous strength in each 40 meV linewidth for nuclear absorption in the materials to be tested. Over a hundred such pulses per second can be produced with the existing device.

TABLE III

IRRADIATION DEVICES ONLINE IN 1986

	AV. POWER (Watts)	CONTINUUM (Photons/sec/0.1%BW)	EQV. ACTIVITY (kCi/0.1%BW)
EXRAD	0.03	1.9 X 10[illegible]	500
FALCON	0.3	2 X 10[illegible]	3000
GEMINIX (Two FALCON modules)	0.6	4 X 10[illegible]	6000

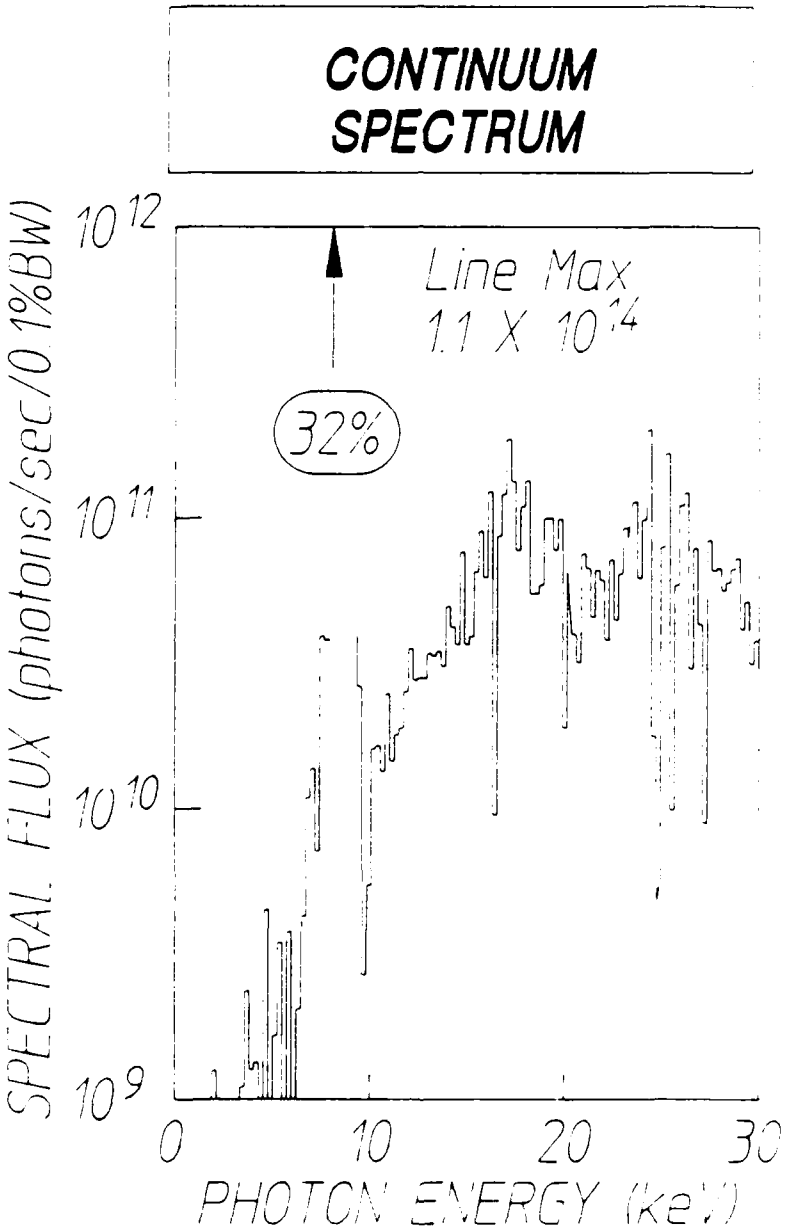

Figure 18: Typical spectral distribution of flux emitted from the scale 0.33 device.

For comparison the largest synchrotron yet designed (ALS) is projected to give 0.86 Ci simultaneously into each of the much more restricted range of linewidths generating a total of only 0.22 MegaCuries per pulse. More pulses per second can be produced than can be used because the fluorescence of a material under test must be allowed to decay before a new pulse can be introduced. Generally the usable repetition rates cannot be high enough to offset the lower intensities so that while the ALS will be 1000 times more expensive it will not be as effective a source as our flash x-ray device for characterizing the "kinetics" of candidate materials for a gamma-ray laser.

Our current plan of work projects the construction of a constellation of FALCON-scale devices, synchronized to produce a total strength approaching a kiloCurie per line. A scheduled increase in operating voltages would extend coverage over the full range 3-100 keV.

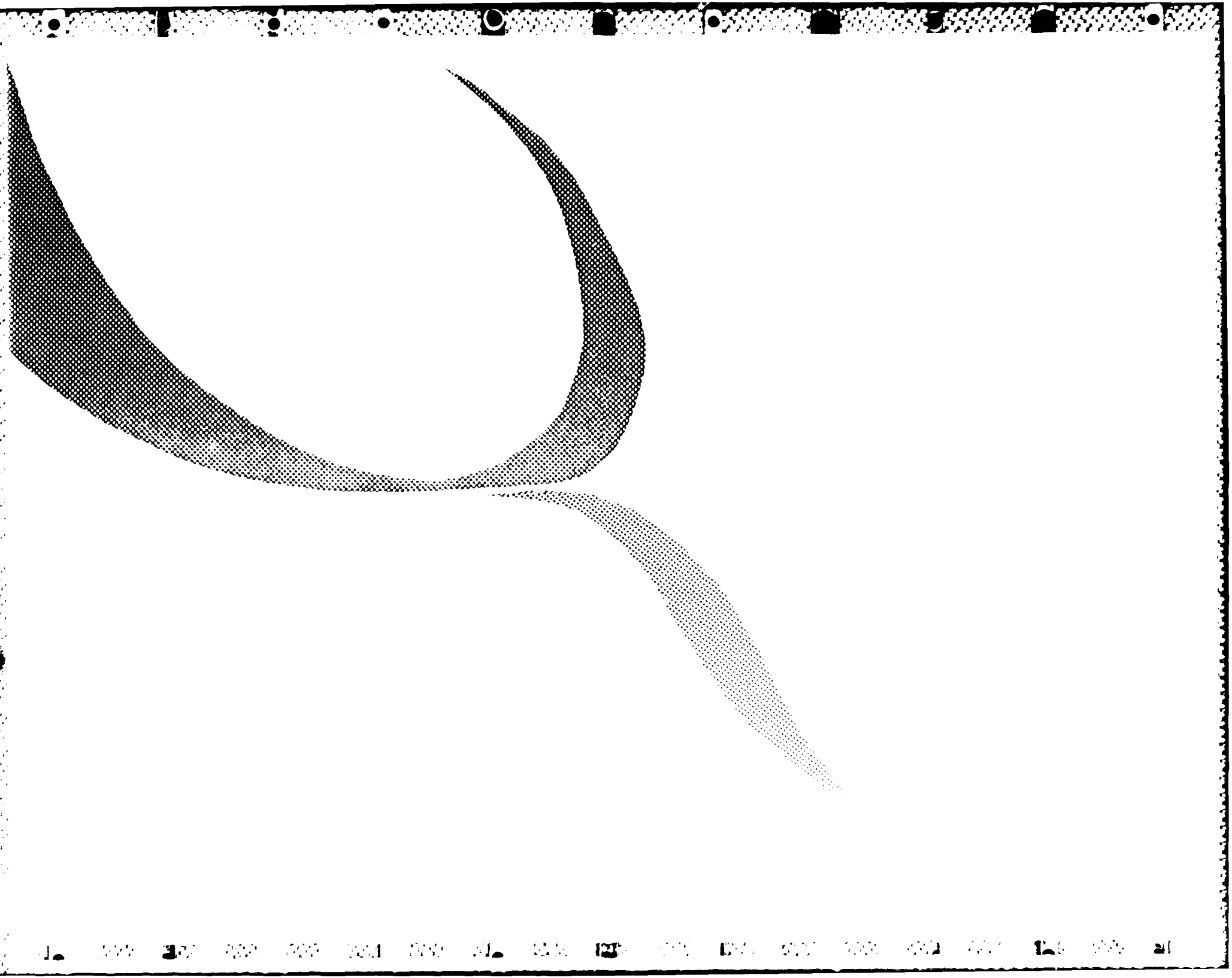

FREQUENCY MODULATION SPECTROSCOPY

S.S. Wagal, P. Reittinger, and C.B. Collins

Basic Concepts and Phenomenology

Most laboratory sources of gamma radiation emit at levels of intensity corresponding to single photon conditions. Mossbauer experiments, for example, are rarely conducted at such great intensities that the detection of two photons would be probable in the transit time spent between source and absorber. Under those conditions the perception of gamma rays as streams of particles is instinctive. Nevertheless, as elements of electromagnetic radiation they must also be considered as carrier waves of high frequency. Early in the development of Mossbauer spectroscopy, the frequency modulation of such gamma-ray "carriers" was demonstrated by Ruby and Bolef in a classical experiment.[1] By imposing periodic Doppler shifts of purely mechanical origin upon a Mossbauer source in a simple transmission experiment, they developed sum and difference frequency spectral lines displaced from the normal gamma-ray carrier frequency by integral multiples of the mechanical frequency. In fact they produced sidebands on their gamma-ray spectral lines

In the late 1960's Mitin[2,3] reported a theory which predicted that sidebands of an equivalent appearance could be generated by exciting the Mossbauer transitions as part of a multiphoton process in nuclei immersed in intense radiofrequency (rf) fields. This similarity of effects arising from such different origins provided the basis for years of critical controversy which continues to the present time. Because our coherent pumping scheme has a generic relationship to the original Mitin proposal, we inadvertently inherited some of this arcane controversy. Unfortunately, several of the early experiments were flawed by the technological and conceptual limitations of the times, and it was necessary for us to focus considerable effort this past quarter upon a reexamination and extension of the critical experiments which had launched the original controversy.

The earliest actual experiment in radiofrequency sideband production, reported by Perlow[31] in 1968, focused upon the components of the 14.4 keV transition in ^{57}Fe. Several ^{57}Co sources diffused into ferromagnetic hosts were immersed into intense magnetic fields oscillating at radiofrequencies. Those results were explained[31] as the magnetodynamic modulation of the hyperfine fields and generally conformed to the Mitin hypothesis for multiphoton transitions. Two of the three groups who initially documented this phenomenon favored the magnetodynamic explanation which required no mechanical action,[31,32,33] while the other group began to develop an alternative based upon magnetostriction.[34,35] Most of the actual experiments had used ferromagnetic hosts to enhance the applied magnetic fields, and such materials are almost invariably magnetostrictive. In the model finally synthesized, the same type of periodic Doppler shifts of Ruby and Bolef[28] were assumed to be driven by acoustic phonons which were excited by magnetostriction along the greatest dimensions of the material and scattered onto the axis connecting source and absorber. To be effective this mechanism required the sample to have a large acoustic Q so that displacements of the active nuclei could build to significant values.

Despite the accretion over the years of a large body of phenomenology presumed to describe rf sidebands on Mossbauer transitions, the magnetostrictive-acoustic theory never quantitatively predicted the amplitudes of the sidebands as functions of either applied power or frequency. However, the magnetodynamic models of that early time fared no better, and attention unfortunately turned to "proving" a magnetostrictive origin by distressing the alternative explanations.[36] The obvious difficulty with proving a theory by distressing the alternatives is that those other explanations may not have reached comparable levels of maturation. The magnetodynamic models of the late 60's were relatively easy to destroy. However, the recent successes of ferromagnetodynamics[37,38] show the early models[31] of sideband formation to have been inspired, but inadequate approximations. Their failures to withstand the stresses of the Pfeiffer experiments[36] can be readily seen in hindsight to be neither surprising nor significant. Those models simply did not embody the level of sophistication necessary to describe the complex switching behavior of magnetization in ferromagnetic foils subjected to various combinations of static and oscillating fields in those geometries employed. It is now accepted[37,38] that in such geome-

tries oscillating fields are produced by the various precessions that have substantial components, H_j normal to the major faces.

From current perspective it is the benchmark experiment reported by Chien and Walker[33] that forms the bulwark of the magnetostrictive-acoustic explanation of Mossbauer sidebands. In that finely executed experiment, an absorbing foil composed of ferromagnetic and nonmagnetic layers was used to study transport of the causitive agent from the ferromagnetic layer into the nonmagnetic, where sidebands were produced upon Mossbauer transitions of embedded ^{57}Fe nuclei. Very clear evidence showed:

1) that cause did arise in the ferromagnetic Ni layers, producing sidebands only in the nonmagnetic stainless steel layers.
2) that tight coupling between layers favored the excitation of sidebands and poor coupling attenuated it.

These results seemed conclusive in demonstrating the cause as a transport of phonons from one layer to the next with a high acoustic [illegible]. These experiments were repeated in the work reported here, but with extensions which seem to contradict the classic interpretation.

Three experiments were conducted in this past quarter. The first was designed to elaborate upon the Chien and Walker demonstration of the importance of tight coupling and high acoustic [illegible].

Although not unique for all sidebands in a spectrum, the [illegible] modulation index, m as a measure of the strength of the development of the sidebands offers practical convenience for description. For a magnetostrictive origin

$$m = x_j / \lambda, \qquad (1)$$

where x_j is the amplitude of the periodic displacement of the nuclei and $\lambda = 0.137$Å for the 14.4 keV line of ^{57}Fe. In the correspondence [illegible] dynamic model,

$$m = bH, \qquad (2)$$

where H is the applied magnetic field and b provides the [illegible] between H_j and H. For relatively small m, at which [illegible] is negligible, the ratio of the magnitude of the first sideband [illegible]

intensity in the original parent line is proportional to [illegible] which in turn is proportional to P, the applied radiofrequency power.

One of the most compelling results presented by Thiem and Weaver was a demonstration of the enhancement of m attributed by tighter acoustic coupling of layers. They found that electroplating Ni upon a stainless steel foil produced much higher values of m in absorption experiments than could be obtained by gluing a Ni foil to the stainless foil. They attributed the difference to the obviously poorer acoustic properties of the glue. However, as part of this report we observe that their stainless foil was electroplated on both sides with Ni while the epoxied bond was used to join a single Ni foil to one side of the stainless absorber. While the m defined by Eq. (9) could not be additive if produced in different magnetostrictive layers, in principle the H_j upon which m depends in Eq. (10) could add coherently. Two sources of m arising from distinctly separate sources could give a resulting modulation of $4m^2$ in a magnetodynamic model. This is about the magnitude seen in the data of Ref. 39 of the difference that resulted from excitation with two electroplated layers in comparison to excitation from one glued layer.

In our first experiment we observed that simple contact of two Ni driving layers with an enriched stainless foil between them seemed to provide as favorable coupling as did electroplating. Moreover, we found that the transfer of the agent of excitation could be accomplished over considerable distance through materials with exceedingly poor acoustic properties. Figure 19 depicts to scale the most extreme arrangement in which a 2.0 μm thick stainless steel absorber foil was wrapped with a 100 μm cushion of facial tissue and then placed between two, 2.5 μm thick Ni driver foils. Microscope cover slides on the outer surfaces of the Ni foils provided mechanical strength. The insets show the essential results. In Fig. 19a no sidebands are seen in the absence of applied power and in Fig. 19b sidebands are evident at 6 watts of power into the coil containing the assembly in a resonant circuit of electrical Q of 113 at 22 MHz. Perhaps it is possible to imagine transport of phonons in such a system, but it should be noted that the tissue was composed of random arrays of fibers with diameters considerably smaller than a wavelength for a vibration at these frequencies, characteristics presumed in the literature[35,36] to provide a reasonable barrier to the transfer of vibration.

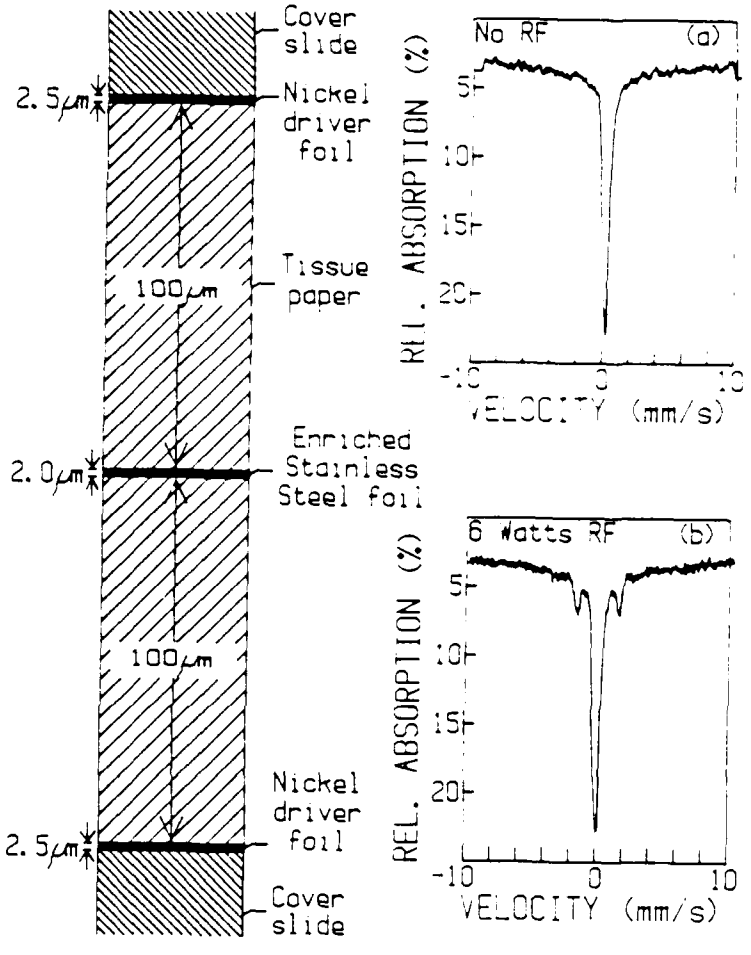

Figure 19: A scaled figure of the foil arrangement designed to insulate the ^{57}Fe enriched stainless steel absorber from phonons arising in the Ni foils. Figure 19a) shows that a single line absorption spectrum is obtained from the foil arrangement when no rf field is applied. Figure 19b) shows that sideband absorptions can be induced in such a mechanically isolated absorber foil.

In a second experiment we explored the additivity of the effects contributed by independent sources. The same stainless absorber foil used in the first experiment was tightly sandwiched between two Ni foils each 2.5 μm thick. The Ni foils had been cut from a single sheet of polycrystalline nickel, supposed not to have been magnetically textured. We assumed that the magnetic easy axes in each component crystallite to be randomly oriented. A cursory examination showed the effect of two identical foils injecting excitation from both sides was simply twice the effect obtained with one foil on one side. In effect the values of m^2 being communicated by each single foil were additive yielding a modulation index of $2m^2$ from the pair. As expected, both the transferred displacements, x_0 and the m resulting from the fields H appearing in Eqs. (9) and (10), respectively, were only randomly correlated between the two distinct sources.

When the foil assembly was biased with a static magnetic field applied in the plane of the foils but perpendicular to the oscillating magnetic field, completely different results were obtained. Figure 20a shows the dependence of the size of the first order sidebands upon power applied to the two Ni foils in order to establish a measure of linearity. Spectra were scaled so that the transition probability remaining in the central peak was constant as a convenience to minimize distortion resulting from saturation of the near-linear dependence of first order effects upon power. In this way m^2 could be more readily visualized as being nearly proportional to sideband amplitude. However, values actually shown were computed according to the prescription of Ref. 39.

Figure 20b shows the comparison between the effect of one source of excitation with that from two when both were biased with the static field. In obtaining data for this comparison the product of rf power, P and electrical Q of the circuit containing the solenoid with the foil was maintained constant. Elementary analysis shows that if PQ is constant, the rf current in the solenoid in such a circuit is also constant and hence the two arrangements are subjected to the same solenoidal rf field. In this case the modulation index obtained with the two driver foils can be seen to be $3.2m_s$, where m_s is the index produced by a single one of the foils. While it is inconceivable that the localized values of the x_0 from separate foils could become correlated, it is possible that the m in Eq. (10) could

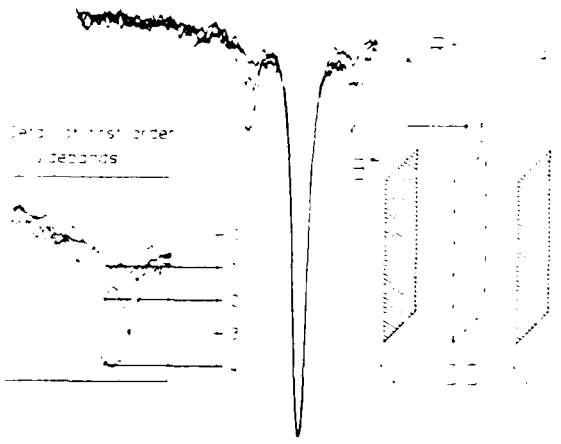

Figure 20a: An ^{57}Fe enriched stainless steel foil (SS) was sandwiched between two Nickel driver foils (Ni) and placed in mutually perpendicular static and rf B-fields. Three different absorption spectra were obtained with 1 Watt, 2 Watts, and 4 Watts of power of the applied rf. The three spectra are scaled such that their central peaks are of a constant height. Using the fact that the first order sidebands scale linearly with the power of the applied rf, a linear scale was derived from the heights of these sidebands assuming a ratio of 1:2:4 (refer to inset).

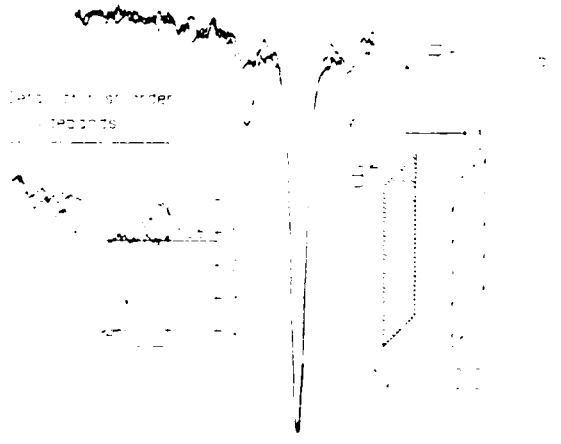

Figure 20b: An enriched stainless steel foil with a single Nickel driver foil was placed in mutually perpendicular static and rf B-fields. The power of the applied rf was 4 Watts. The spectrum thus obtained is plotted along with the spectrum obtained with two Nickel driver foils at 4 Watts rf so that their central peaks are of a constant height. The first order sideband from the single driver arrangement was then measured relative to the scale derived in Figure 20a. It is seen that the ratio of the intensities of the first order sidebands produced in a foil driven on one side to those produced in a foil driven on two sides is about 1 : 2 (refer to inset).

The bias would insure that the rocking of the saturation field in each crystallite started in the same hemisphere as the rf fields commenced each cycle of oscillation. This would insure partial correlation of the normal components of the magnetic fields transferred from the two separate foils.

In a third experiment we attempted to determine whether the modulation index, m, scaled with the magnetostrictive properties of the driver or with its permeability; in essence whether m was more appropriately given by Eq. (9) or Eq. (10). In this sequence the same stainless absorber foil was first wrapped in a single foil of natural iron 0.2 mm thick and then sandwiched in graphite plates rather than the microscope slides. Data shown in Fig. 21a were obtained when this sample was driven by 17.0 W of radiofrequency power applied to the resonant circuit containing the coil, with the Q-factor arranged to be 17.5. Sidebands up to the fifth order can be clearly seen. For comparison the spectrum obtained for the stainless foil in the fields but without the driver is shown in Fig. 21c, and the spectrum of the natural iron wrapper in the rf fields is shown in Fig. 21d. In the latter case the overlapping and blending of line and sideband components at this frequency can be seen to produce no appreciable structure in agreement with previous observations.

Figure 21. Spectra obtained with absorber foil arrangements in a 15MHz Rf B field at a power of 17 Watts.

a) ^{57}Fe enriched stainless steel foil enveloped by a natural Fe driver foil.

b) ^{57}Fe enriched stainless steel foil enveloped by a ^{56}Fe driver foil.

c) ^{57}Fe enriched stainless steel only.

d) Natural Fe driver foil from a.

Nickel has a much larger magnetostrictive constant than iron, the comparison being -30.0 to 5.0 in customary units.[7] Data shown in Fig. 21b were obtained by replacing the iron foil driver with a nickel foil 2.5 μm thick, wrapped around the same absorber in the same manner. The literature[7] is unanimous in attributing larger sidebands to thinner drivers so the more substantial development of sidebands with the iron foil driver seen in Fig. 21a and 21b completely contradicts a simple magnetostrictive origin of the effect.

While confirming the experimental results of the landmark Olsen and Walker paper, these new results go beyond the preparation to test at that time and display behaviors completely inconsistent with the traditional magnetostrictive-acoustic origin of Mossbauer sidebands. Recently it has been reported[8-10] that in some arrangements the sideband intensities developed by rf fields on Mossbauer transitions can be quantitatively explained with a multiphoton model based upon the dressed state theory of Cohen-Tannoudji.[11] The sidebands in these experiments were perceived as arising from gamma-ray transitions between nuclear states whose energies had been shifted by integral multiples of the quanta of the electromagnetic field dressing the particle states. In view of the successes of that particular magnetodynamic model in these circumstances and these new results contradicting the conclusions of the Olsen and Walker[3] experiment, it would appear that the controversy over the origin of Mossbauer sidebands cannot yet be considered resolved.

It is most reasonable to expect that some combination of magnetodynamic and acoustic causes can provide a comprehensive explanation of all of the complex accretion of phenomenology to which we have added these new aspects, but further work will be needed to determine under what circumstances one or the other dominates. Such experiments continue to lie at the focus of our activities along these lines.

Instrumentation of FMS

The sum and difference frequency sidebands produced on intrinsic Mossbauer transitions has made possible very effective new instrumentation for high resolution spectroscopy at gamma-ray energies. A prototype version of this Frequency Modulation Spectrometer (FMS) was first described[12] by our laboratory in 1985 and subsequent refinements were made with support from an earlier ONR Contract followed by work performed during this reporting period. This device monitors changes in the intensity of transmitted single-frequency gamma photons as a function of frequency of the long wavelength photons of the alternating magnetic field in which the absorbing nuclei are immersed.

At the heart of it is a multi-channel scalar (MCS) and IEEE-488 GPIB interface with an Apple II+ computer (Fig. 22). The MCS was designed to have a 100% duty cycle. The GPIB enables the spectrometer to sweep continuously through the frequencies of an rf magnetic field with a Wavetek frequency synthesizer. The Mossbauer drive allows the frequency of the gamma photon to be biased by a constant Doppler shift, if desired. The spectrometer in its present form has an instrumental resolution of 100 Hz and a range of 10^3 Hz with a stability of 0.1 Hz/sec with a stationary source. These characteristics are comparable to having a Mossbauer spectrometer with a means of Doppler shifting the gamma-ray source with a resolution of 10 nm/sec and a range of 100 nm/sec with a stability of 0.01 nm/sec/sec.

In operation FMS of ^{57}Fe provides a direct measurement of rf sideband positions and intensities, from which one can extrapolate information about the transitions between Zeeman split energy levels (parent transitions), labeled 1 through 6 in Fig. 23. Rf sidebands have been labeled as a parent transition preceded by a number of +'s or -'s, the number of which corresponds to the number of rf field energy quanta (order of the sideband) added to or subtracted from the parent transition. The symmetrically opposed parent transitions 1 and 6 are separated by 123.7 MHz. Applying a 61.85 MHz alternating magnetic field to the Fe foil produces (+1) and (-6) sidebands which overlap in the symmetric center, or transition center, of the hyperfine structure of the ^{57}Fe

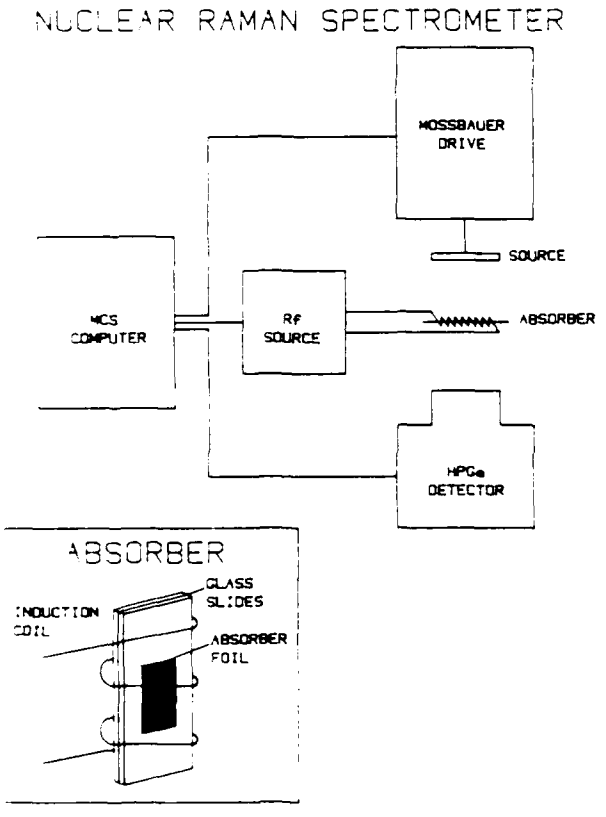

Figure 22. Automated FMS.

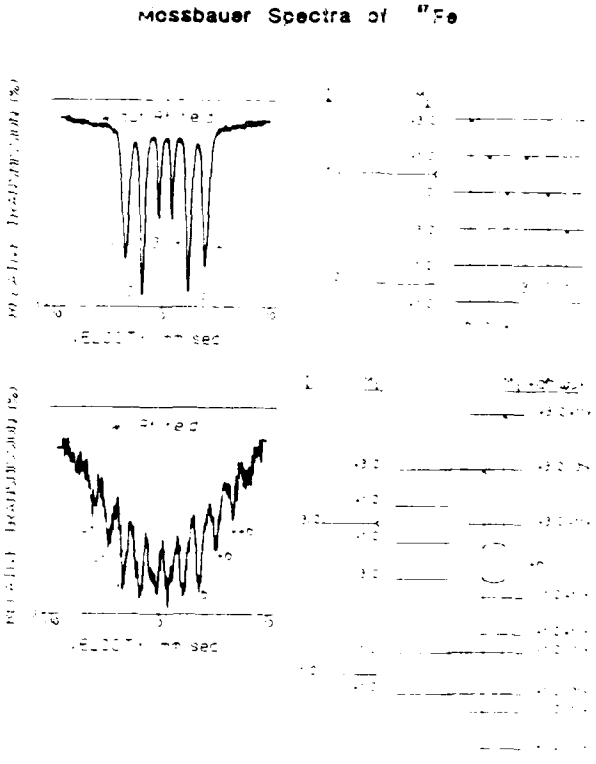

Figure 23. Mossbauer spectra of Fe foil.

The energies of the gamma ray emitted by the source and the transition center of the absorber differ by the isomer shift, Δ (Fig. 24a). In FMS the Stokes sideband from parent transition 6, (-6), would be detected at a frequency of (61.85-Δ) MHz while the anti-Stokes sideband from parent transition 1, (+1), would be detected at a frequency of (61.85+Δ) MHz (Fig. 24b and c). Therefore, FMS should produce a spectrum with two peaks around 60 MHz, separated by 2Δ.

If we apply a small Doppler shift, δ, to the source, we should obtain an FMS spectrum with two peaks around 60 MHz, separated by $2(\Delta +$ (Fig. 25).

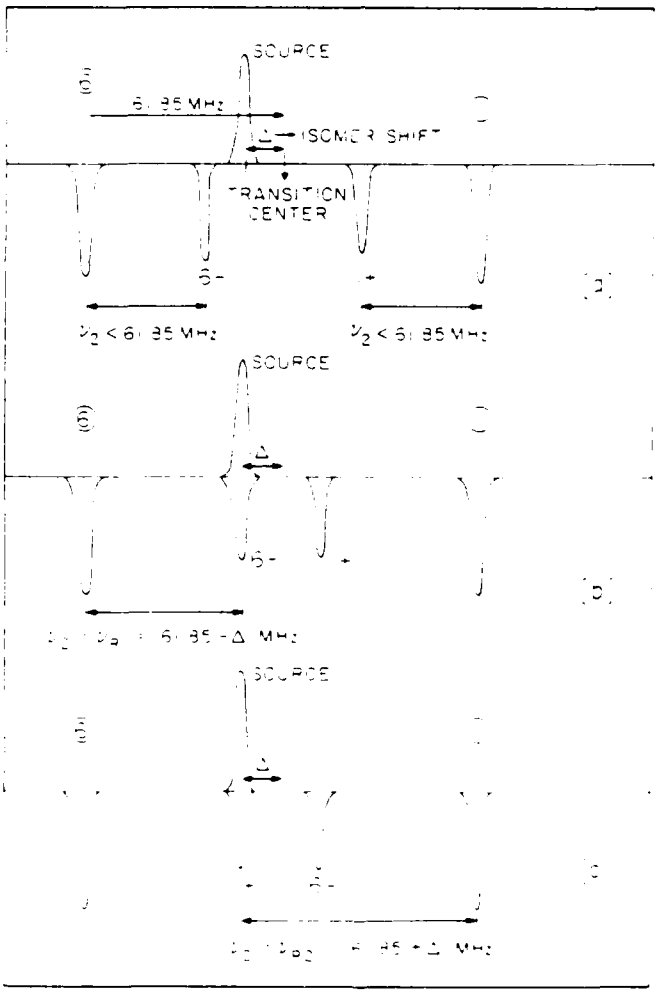

Figure 24. How FMS measures isomer shift.

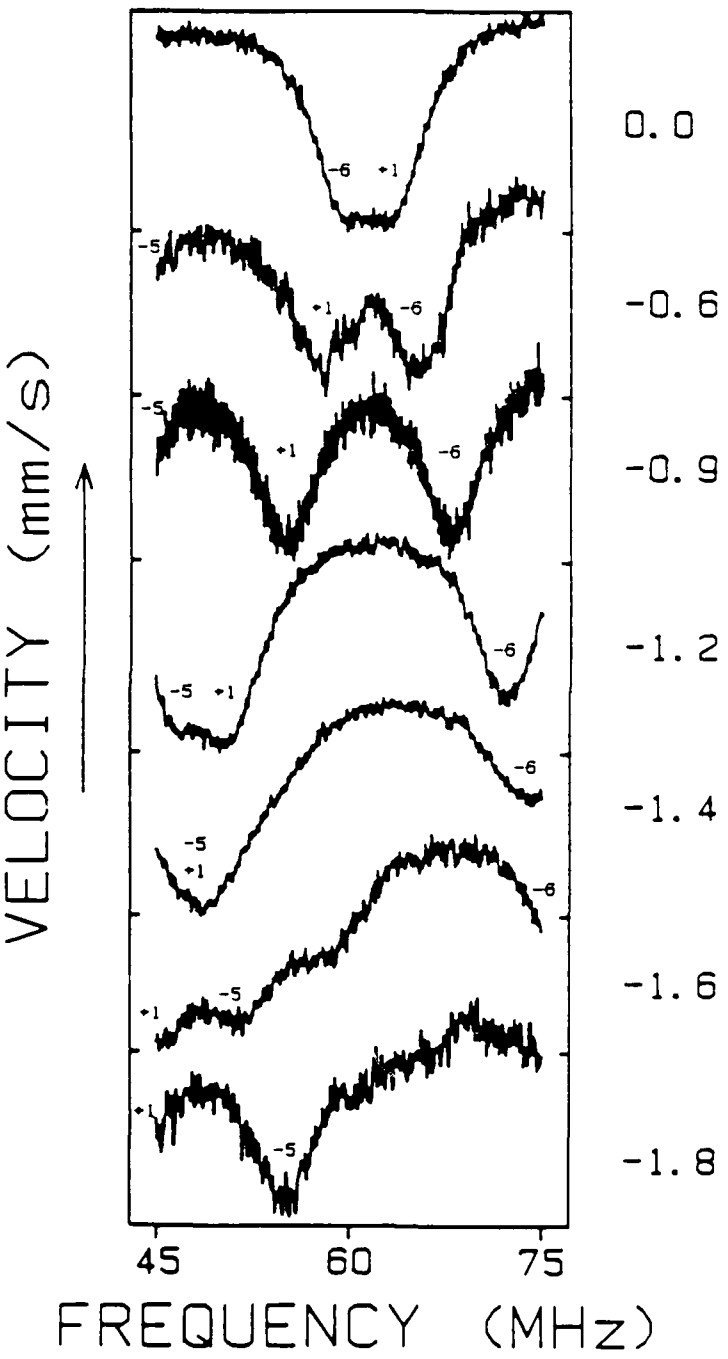

Figure 25: Typical FMS spectra.

Classically, the frequencies at which sidebands appear, fs, is simply

$$fs(MHz) = [\ v - (P_j + iso)] * (11.6/ord), \qquad (11)$$

where P_j is the position of the j'th parent transition (mm/sec), v is the velocity of the source (mm/sec), iso is the isomer shift (mm/sec), and ord is the order of the sideband of interest. The source used was in a Pd lattice (iso = -0.185).

Rf sideband positions are also apparently affected by the intensity of the rf magnetic field (Fig. 26). It is yet to be determined whether sideband position is a function of intensity as well as frequency of the rf magnetic field, or whether the temperature shift of the parent transitions is being detected, or both. Since we start with a negative isomer shift, raising the temperature of the absorber should reduce the energy difference between the source transition and the transition center of the absorber. Therefore, increasing the rf field intensity should raise the temperature of the absorber and in turn decrease the isomer shift.

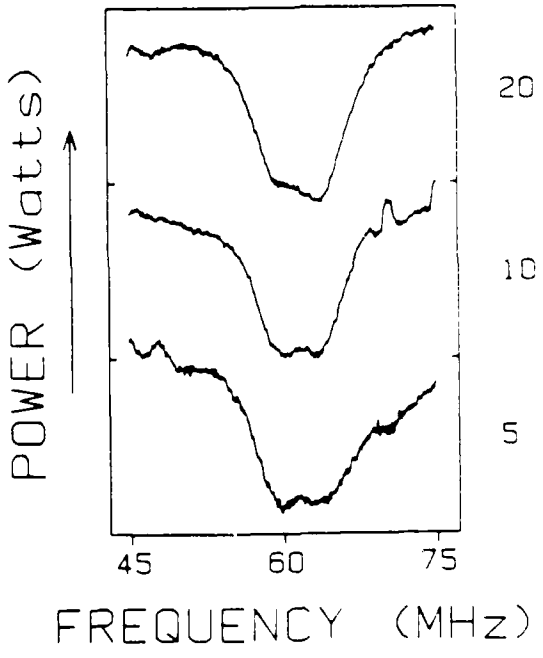

Figure 26: Effect of field intensity on sideband position.

It seems clear that, in addition to providing information about sideband intensity and position, FMS could also prove to be a means for direct and accurate measurement of isomer and temperature shifts, spectroscopic quantities that are difficult to measure with Mossbauer spectroscopy as usually practiced because of the difficulty in obtaining such small velocities with such precise control. For the purposes of the gamma-ray laser program it is the combination of narrow instrumental width and large tuning range that offers the greatest attractions.

To dress an isomeric state requires a certain arrangement of nuclear levels that would make them undetectable to conventional techniques of nuclear spectroscopy. Our method of FMS is the only means found to date that can be used to search for this combination among the 29 best candidates. The successes of the new FMS apparatus for nuclear spectroscopy indicate that a much higher resolution, by perhaps several more orders of magnitude, can be achieved through a reasonable upgrade of the apparatus. If the range of tunability does extend to the ferromagnetic spin resonance (FSR) frequency, then it will be possible to construct a swept frequency device capable of continuously tuning over a range of 10^{4} line-widths, an enormous improvement in the state-of-the-art of nuclear spectroscopy.

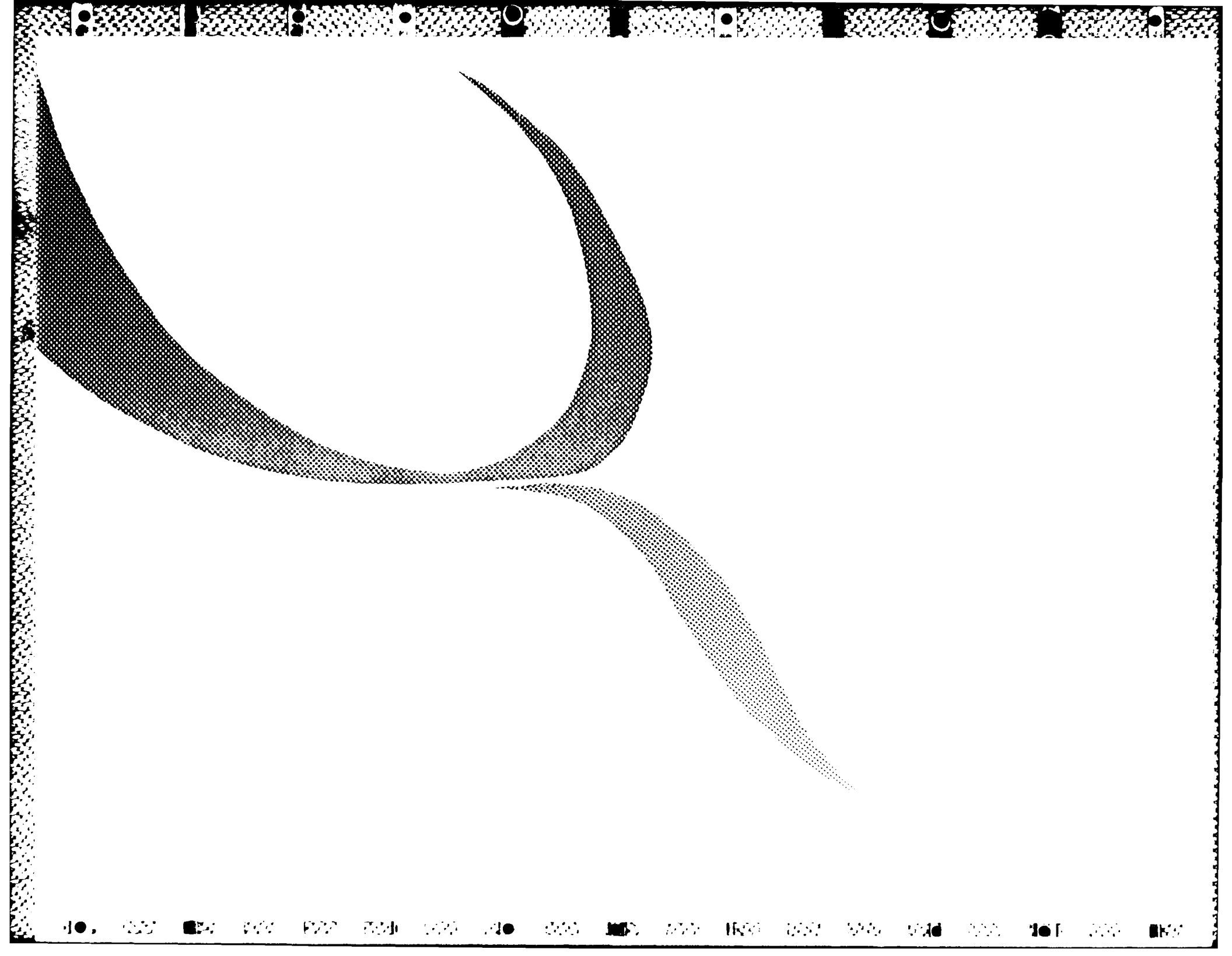

REFERENCES

1. C. B. Collins, S. Olariu, M. Petrascu, and I. Popescu, Phys. Rev. Lett. 42, 1397 (1979).
2. C. B. Collins, S. Olariu, M. Petrascu, and I. Popescu, Phys. Rev. A 20, 1942 (1979).
3. S. Olariu, I. Popescu, and C. B. Collins, Phys. Rev. A 23, 53 (1981).
4. S. Olariu, I. Popescu, and C. B. Collins, Phys. Rev. C 23, 1007 (1981).
5. C. B. Collins in Proceedings of the International Conference on Lasers '80, edited by C. B. Collins (STS Press, McLean, VA, 1981) p. 524.
6. C. B. Collins in Laser Techniques for Extreme Ultraviolet Spectroscopy, edited by T. J. McIlrath and R. R. Freeman (AIP Conference Proceedings No. 90, New York, 1982) p. 454.
7. C. B. Collins in Proceedings of the International Conference on Lasers '81, edited by C. B. Collins (STS Press, McLean, VA, 1982) p. 291.
8. C. B. Collins, F. W. Lee, D. M. Shemwell, B. D. DePaola, S. Olariu, and I. I. Popescu, J. Appl. Phys. 53, 4645 (1982).
9. B. D. DePaola and C. B. Collins, J. Opt. Soc. Am. B 1, 812 (1984).
10. C. B. Collins and B. D. DePaola in Laser Techniques in the Extreme Ultraviolet, edited by S. E. Harris and T. B. Lucatorto (AIP Conference Proceedings No. 119 New York, 1984) p. 45.
11. C. B. Collins and B. D. DePaola, Optics Lett. 10, 25 (1985).
12. B. D. DePaola, S. S. Wagal, and C. B. Collins, J. Opt. Soc. Am. B 2, 541 (1985).
13. C. B. Collins in Advances in Laser Science-1, edited by W. C. Stwalley and M. Lapp (AIP Conference Proceedings No. 146, Dallas, 1985) p. 18.
14. F. Davanloo, T. S. Bowen, and C. B. Collins in Advances in Laser Science-1, edited by W. C. Stwalley and M. Lapp (AIP Conference Proceedings No. 146, Dallas, 1985) p. 60.
15. S. S. Wagal and C. B. Collins in Advances in Laser Science-1, edited by W. C. Stwalley and M. Lapp (AIP Conference Proceedings No. 146, Dallas, 1985) p. 62.
16. C. B. Collins in Advances in Laser Science-1, edited by W. C. Stwalley and M. Lapp (AIP Conference Proceedings No. 146, Dallas, 1985) p. 40.

17. G. C. Baldwin, J. C. Solem, and V. I. Goldanskii, Rev. Mod. Phys. 53, 687 (1981).
18. C. Cohen-Tannoudji and S. Haroche, J. de Physique, 30, 125 (1969).
19. S. Haroche, Ann. Phys. 6, 189 (1971).
20. C. B. Collins, Expansion of Research on the Tuning and Stimulation of Nuclear Radiation, University of Texas at Dallas, Report #GRL-01, Office of Naval Research, October 1986.
21. W. J. Veigele, Atomic Data Tables, 5, 51 (1973).
22. C. B. Collins, F. Davanloo, and T. S. Bowen, Rev. Sci. Instrum. 57, 863 (1986).
23. L. C. Bradley, A. C. Mitchell, Q. Johnson, and I. D. Smith, Rev. Sci. Instrum. 55, 25 (1984).
24. Q. Johnson, A. C. Mitchell, and I. D. Smith, Rev. Sci. Instrum. 51, 741 (1980).
25. D. Attwood, Science 228, 1265 (1985).
26. C. B. Collins, IEEE J. Quantum Electron. QE-20, 47 (1984).
27. Peter Krehl, SPIE Review 689, 26 (1986).
28. S. L. Ruby and D. I. Bolef, Phys. Rev. Lett. 5, 5 (1960).
29. A. V. Mitin, Sov. Phys. JETP 25, 1062 (1967).
30. A. V. Mitin, Sov. Phys. Dok. 15, 827 (1971).
31. G. L. Perlow, Phys. Rev. 172, 319 (1968).
32. G. Asti, G. Albanese, and C. Bucci, Il Nuovo Cimento 57B, 531 (1968).
33. G. Asti, G. Albanese, and C. Bucci, Phys. Rev. 184, 260 (1969).
34. N. D. Heiman, L. Pfeiffer, and J. C. Walker, Phys. Rev. Lett. 21, 93 (1968).
35. N. D. Heiman and J. C. Walker, Phys. Rev. 184, 281 (1969).
36. L. Pfeiffer, N. D. Heiman, and J. C. Walker, Phys. Rev. B 6, 74 (1972).
37. T. H. O'Dell, Ferromagnetodynamics (Wiley, New York, 1981), Chap. I.
38. C. W. Chen, Magnetism and Metallurgy of Soft Magnetic Materials (North-Holland, Amsterdam, 1977).
39. C. L. Chien and J. C. Walker, Phys. Rev. B 13, 1876 (1976).
40. Richard M. Bozorth, Ferromagnetism (D. Van Nostrand Company, 1951).
41. B. D. DePaola, Experimental Studies of the Interaction of the Nucleus with Long Wavelength Radiation, (unpublished Ph.D. Thesis, University of Texas at Dallas, 1984), p. 18.

APPENDIX

CENTER FOR QUANTUM ELECTRONICS
UNIVERSITY OF TEXAS AT DALLAS

General Information

The Center for Quantum Electronics was established at the University of Texas at Dallas in 1975 by Professor C. B. Collins, the present director. It was immediately distinguished by the discovery of a new type of visible laser, the charge transfer laser, one of the few new lasers to be invented in a university environment as opposed to being discovered in a national or industrial laboratory. Two years later a patent was issued for another new laser excitation scheme, the repetitively pulsed traveling wave laser. This initial momentum continued to build and in the past five years 33 articles have been published in the reviewed journals detailing our Center's accomplishments.

The central theme in the Center for Quantum Electronics is the development and utilization of new light sources. Over the years this has been expressed through basic research into new spectroscopics, into the use of lasers to create new reactive species, and upon matter in intense fields. A major expansion of activities in the past year, supported by the Innovative Science and Technology Directorate of the Strategic Defense Initiative Office and directed by the Naval Research Laboratory, has been applied to research necessary to determine feasibility of a gamma-ray laser. Our multidisciplinary approach to this problem is unique in joining traditionally-unrelated fields of Quantum Electronics, Nuclear Physics and Solid State Physics. Such a fusion of concepts from different fields of inquiry forms a fertile atmosphere of scientific research and experimentation. It is conservative to say that the realization of a gamma-ray laser would revolutionize both defense and industrial technology.

Currently active within our Center are several interlinked projects supported from a mixture of Federal and local sources. At the cutting edge of emerging technology, these projects offer unexcelled opportunities for the training of students and professionals. For example, eight Ph.D.s have been earned over the past five years under the supervision

of the Director, continuing a trend that has produced a total of 19 Ph.D.s to date. The Center employs 34 staff members, both as research professionals and support personnel. Working on the gamma-ray laser project are 11 Ph.D. students who are doing their dissertations on the experiments they are conducting in connection with this project.

Located at the north periphery of the campus at UTD, the Center for Quantum Electronics occupies 10,500 square feet in adjoining buildings. A unique flash x-ray lab under construction will consist of 16 pulsed-power transmission lines, each 16 feet long, converging on a target chamber where the candidate laser materials will be tested. This 3,600 square-foot facility is one of two projects under active construction at this time. Including remodeling projects to outfit existing buildings on campus to the specific needs of the research in progress, the Center for Quantum Electronics expects to add almost 6,000 additional square feet before the end of the year.

January 1987

END

4-88

DTIC